Shallow subsurface thermal structure onshore Denmark: temperature, thermal conductivity and heat flow

INGELISE MØLLER, NIELS BALLING & CLAUS DITLEFSEN

Møller, I., Balling, N. & Ditlefsen, C. 2019. Shallow subsurface thermal structure onshore Denmark: temperature, thermal conductivity and heat flow. © 2019 by Bulletin of the Geological Society of Denmark, Vol. 67, pp. 29–52, ISSN 2245-7070. (www.2dgf.dk/publikationer/bulletin). https://doi.org/10.37570/bgsd-2019-67-03

Received 9 November 2018
Accepted in revised form
12 March 2019
Published online
5 June 2019

Two supplementary
data files

Available measured temperatures and thermal conductivities covering Danish onshore areas to a depth of about 300 m have been compiled and analysed. Temperature data from 236 borehole sites, including 56 boreholes with detailed temperature profiles, are applied together with thermal conductivities mea-sured on samples collected at 34 well-characterised outcrops and on core material from 20 boreholes.

Significant thermal variations in the shallow subsurface are observed. At a depth of 50 m, a mean temperature of 8.9 ± 0.8°C is found, close to the mean annual surface temperature. Higher mean values of 9.7 ± 1.1°C found at 100 m and 11.6 ± 2.2°C at 200 m reflect a general increase of temperatures with depth. In contrast to the assumption commonly held, we observe significant lateral variations both locally and regionally. At a depth of 100 m, temperatures vary between 7.3 and 13.0°C across Denmark, and at 250 m between 9.6 and 17.9°C.

Mean values of the thermal conductivities lie within a range of 0.6–6 W/(m·K) measured water-saturated at laboratory conditions. The majority of values are within the interval of 1–3 W/(m·K) and show a strong correlation with lithology. The content of quartz and the rock porosity (the content of water) are found to be two main factors controlling the observed variations. Characteristic temperature gradients are in the range 1–4°C/100 m. Following Fourier's law of heat conduction, a clear correlation is observed between temperature gradients and thermal conductivities of different lithologies. Intervals of quartz-rich sand deposits with high thermal conductivity show low temperature gradients, chalk and limestone intervals with intermediate conductivity display intermediate gradients, while sections with fine grained clay deposits of low thermal conductivity show high gradient values. A correlation analysis provides an estimate of regional shallow heat flow of 37 ± 5 mW/m2, consistent with local, classically determined heat-flow values from shallow borehole data. However, it is significantly below deep background heat flow, and this is believed to be caused by long-term paleoclimatic effects.

The shallow subsurface thermal regime across the Danish area is largely controlled by thermal conduction. Only locally, and in rare cases, do we observe temperature perturbations due to groundwater migration. In addition to general geoscientific purposes, our results are important for several applications including exploitation of shallow geothermal energy and the use of the subsurface for heat storage and cooling purposes.

Keywords: Subsurface temperature, thermal conductivity, heat flow, Denmark, shallow depth.

Ingelise Møller [ilm@geus.dk] and Claus Ditlefsen [cdi@geus.dk], Geological Survey of Denmark and Greenland (GEUS), C.F. Møllers Allé 8, DK-8000 Aarhus C, Denmark. Niels Balling [niels.balling@geo.au.dk], Department of Geoscience, Aarhus University, Høegh-Guldbergs gade 2, DK-8000 Aarhus C, Denmark.

Corresponding author: Ingelise Møller.

Subsurface temperatures and thermal properties are important factors in controlling the amount of thermal energy that can be extracted or stored in the ground. Local and regional variations in the thermal conditions affect the design and efficiency of shallow geothermal installations, especially when heat pumps are applied (Rasmussen *et al.* 2016; Sanner 2016). Thus, knowledge about temperature, subsurface thermal properties as well as heat flow are required for estimating geothermal resources and in evaluating methodologies for heat extraction. In contrast to deep geothermal conditions (cf. Balling *et al.* 1992, 2002; Mathiesen *et al.* 2009, 2010), until the present study, the shallow subsurface thermal conditions in Denmark have not been analysed on a national scale.

The first borehole temperatures were measured around 1900 as accurate bottom hole temperatures (Bonnesen *et al.* 1913) while the, at the time, deepest

Danish borehole was drilled at Grøndalseng, Copenhagen. Then about 75 years passed until the 1970s' energy crisis resulted in a beginning exploitation of both deep and shallow geothermal energy. Early studies included high-precision logging of equilibrium temperatures in a number of shallow and deep boreholes, measurements of rock thermal properties on drill cores and outcrop samples as well as estimation of heat flow (e.g. Balling 1979; Balling *et al.* 1981, 1992; Kristiansen *et al.* 1982). Within the last decade, a renewed interest in geothermal energy (e.g. Røgen *et al.* 2015), driven by the needs for CO_2 neutral energy sources, have stimulated new investigations and provided new information on subsurface thermal conditions (e.g. Vangkilde-Pedersen *et al.* 2012; Ditlefsen *et al.* 2014; Balling *et al.* 2016; Poulsen *et al.* 2017; Weibel *et al.* 2017; Erlström *et al.* 2018; Major *et al.* 2018).

In this paper, all available data on shallow subsurface thermal conditions, old and new, published as well as unpublished, have been compiled and analysed with the main purpose of providing detailed information on the temperature field, temperature gradients and thermal conductivity of the main lithologies. The study covers onshore areas to depths of about 300 m, thus including different sediments from Maastrichtian chalk over Palaeogene limestone and clay, Neogene sand and clay to Quaternary glacial sediments, as well as older sediments and rocks from the island of Bornholm. Since rock thermal properties and temperature gradients are closely related to lithology, the sampled intervals are divided into general litho-chronological groups.

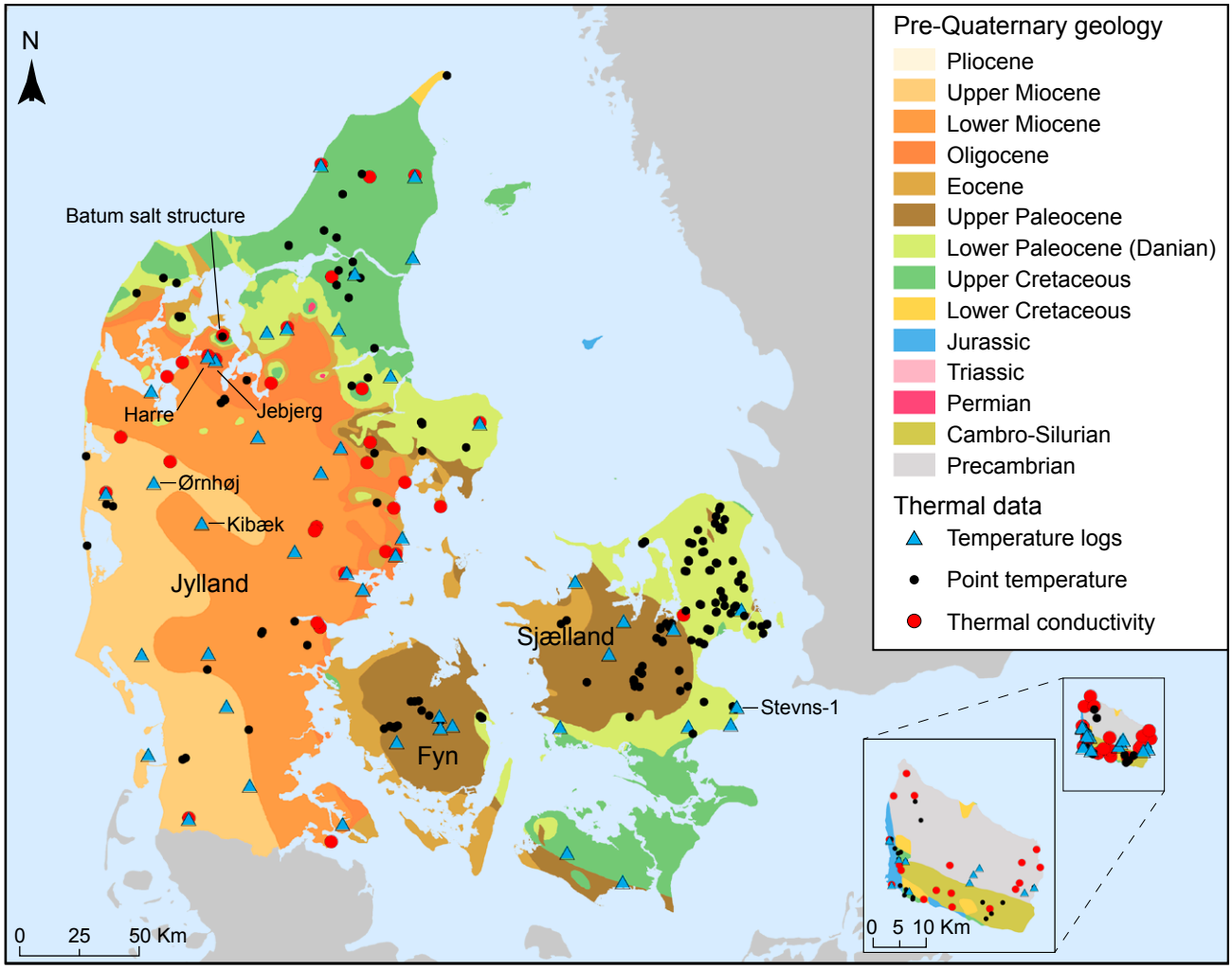

Fig. 1. Location of the applied shallow subsurface thermal information: boreholes with temperature data and sites of thermal conductivity measurements. The named localities represent boreholes with temperature logs shown in Fig. 3 and Fig. 5 as well as the Batum salt diapir which presents anomalous thermal conditions. The background map shows the age distribution of the uppermost Pre-Quaternary substratum, after Håkansson & Pedersen (1992).

Geological setting and lithologies

The shallow subsurface in Denmark primarily consists of sediments spanning from Cretaceous chalk, Palaeogene limestone, marls and clays, Neogene clay and sand to Quaternary glacial and interglacial deposits. Only at the island of Bornholm, the shallow subsurface consists of crystalline rocks and sediments older than Cretaceous. The Pre-Quaternary sediments (Fig. 1) are covered by varying thicknesses of Quaternary deposits dominated by till and meltwater sediments deposited during a number of glacial periods.

Maastrichtian chalk and Danian limestone are located close to the surface in northern Jylland and eastern Sjælland, while Palaeogene marl and clay deposits are found on central and western Sjælland, on Fyn, and in a narrow belt across Jylland, from the east coast to the western Limfjord area, see Fig. 1. Neogene, marine, deltaic and fluvial deposits of clay, silt and sand are found in central and southern Jylland. On Bornholm, the central and northern part of the island consists of Precambrian gneissic and granitic rocks, and the southern and western rim of the island of Palaeozoic sandstone, shale and limestone as well as Mesozoic sand, silt and clay.

The thickness of the Quaternary cover varies considerably from a few metres in some areas to more than 300 m in northern Jylland and in the deepest buried valleys cutting into the Pre-Quaternary base (Jørgensen & Sandersen 2006; Sandersen & Jørgensen 2017). The sediments are dominated by tills and meltwater deposits of glacial origin intercalated with different interglacial sediments. Postglacial clastic and organic sediments are locally found with considerable thickness.

The sampled succession analysed in this study is divided into main litho-chronological groups, generally following the classification applied in the national geological and hydrological database Jupiter (Hansen & Pjetursson 2011; GEUS 2017), although with somewhat fewer classes, as some units with similar mineral composition, texture and age were combined. The applied litho-chronological groups are listed in Fig. 2. They are used for the statistical analysis of thermal conductivity data as well as the temperature gradient data.

Material and methods

Temperature data

Subsurface temperatures were measured in water-filled boreholes by wireline-logging tools equipped with a thermometer. Measurements in boreholes kept undisturbed may accurately represent true formation temperatures of the surrounding lithologies. However, several factors may cause temperature disturbances. For the present study, undisturbed temperature–depth profiles in thermal equilibrium with the surrounding formations are required. Therefore, disturbances need to be detected to the extent possible. The drilling process, in particular when circulating drilling mud, disturbs the borehole temperature profile, and a certain period of rest after drilling is needed for the borehole to reach thermal equilibrium. Borehole temperatures may also be disturbed by groundwater flow. This may happen within an open well related to pressure differences between permeable levels, e.g. layers or fracture zones. Disturbances may also originate from groundwater flow in aquifers around a well. In this compilation, all temperature data were carefully analysed for any such signs of disturbing factors, to ensure inclusion of only good-quality equilibrium temperatures (see criteria below).

All available borehole temperature data acquired by Aarhus University and GEUS for research purposes, as well as external data reported to the national shallow geophysical database GERDA (Møller *et al.* 2009b) were evaluated, regardless of the purpose of the data acquisition.

Important datasets of particularly high quality originate from temperature logging carried out by the Department of Geoscience, Aarhus University, starting from around 1980. The measurements are from shallow as well as deep boreholes with the main purpose of obtaining high-precision temperature data for heat flow and geothermal energy studies. Early results were reported in Balling *et al.* (1981, 1992) and more recent results, from a deep geothermal well, in Balling & Bording (2013). The data from Aarhus University include published as well as unpublished information from 37 borehole sites, 32 shallow (100 to *c.* 300 m depth) and five deep boreholes. From deep boreholes, only information from the upper 300 m is used. Some boreholes were logged several times, years apart, to see whether temperature equilibrium was established and lately also to investigate possible transient effects from recent climatic change. In most shallow boreholes, temperature data were initially acquired by thermistor probes and discrete point measurements, typically at 5 m depth sampling interval. From the deeper wells, data were acquired using quartz oscillator probes and continuous dense sampling. Older, non-digital data were digitised, and all are included. The sensitivity of the applied temperature probes is better than 0.01°C and the absolute accuracy is generally better than 0.05°C. The construction and measuring principles for both types of probes are described in Balling *et al.* (1981, appendix A1).

Chrono-strat. (Epoch)	Applied litho-chronological groups	Lithology	Lithostatigraphical units	Lithostratigraphical references
Quaternary	Gytja	Organic-rich	E.g. Bælthav Till, East Jutland Till, North Sjælland Till, Mid Danish Till, Kattegat Till, Ristinge Klint Till, Lillebælt Till, Ashoved Till, Treldenæs Till, Tebbestrup Fm, Hedeland Fm	Larsen *et al.* 1977; Jacobsen 1985; Houmark-Nielsen 1988; Larsen *et al.* 2009; Houmark-Nielsen 2004
	Marine sand	Sand, mostly fine, silty and clayey		
	Marine clay	Clay, silty and sandy		
	Meltwater sand/gravel	Sand, mostly medium-coarse, gravelly, silty		
	Meltwater clay	Clay, silty and sandy		
	Sand till	Diamict of sand, gravel and little clay		
	Clay till	Diamict of sand, gravel and more than 12 % clay		
Neogene	Miocene quartz sand/gravel	Sand and gravel, mostly medium-coarse sand, quartz-rich	Marbæk Fm, Gram Fm, Ørnhøj Fm, Hodde Fm, Odderup Fm, Arnum Fm, Bastup Fm, Klintinghoved Fm, Billund Fm, Vejle Fjord Fm, Brejning Fm	Rasmussen *et al.* 2010
	Miocene mica sand	Sand, mostly fine, silty and clayey, mica-rich		
	Miocene mica silt	Silt, clayey, sandy, mica-rich		
	Miocene mica clay	Clay, silty and sandy, mica-rich		
Paleogene	Oligocene clay	Clay, little silt, little mica	Branden Fm, Viborg Fm	Christensen & Ulleberg 1973; Heilman-Clausen 1995
	Søvind marl	Clay, chalk-rich	Søvind Marl Fm	Heilmann-Clausen *et al.* 1985; Heilmann-Clausen 1995
	Eocene clay	Clay	Lillebælt Clay Fm, Røsnæs Clay Fm, Ølst Fm	Heilmann-Clausen *et al.* 1985; Heilmann-Clausen 1995
	Eocene diatomite	Diatomite, some clay	Fur Fm	Pedersen & Surlyk 1983; Heilmann-Clausen 1995
	Paleocene clay	Clay	Holmehus Fm, Æbleø Fm, Kerteminde Marl Fm	Heilmann-Clausen *et al.* 1985; Heilmann-Clausen 1995
	Selandian limestone	Limestone, sandy, glaconite-rich	Lellinge Greensand Fm	Heilmann-Clausen 1995
	Danian limestone	Limestone, bryozoan limestone, chalk	København limestone Fm, Stevns Klint Fm, Faxe Fm, Rødvig Fm	Thomsen 1995
Cretaceous	Maastrictian chalk Campanian chalk	Pure chalk, marly chalk, marl	Møns Klint Fm, Mandehoved Fm	Thomsen 1995; Surlyk *et al.* 2013
	U & L Cretaceous sand/sandstone	Quartz sand (clayey, glaconitic)	Bavnodde Grønsand Fm, Anager Grønsand Fm, Jydegård Fm, Robbedale Fm, Rabekke Fm	Gravesen *et al.* 1982
	U & L Cretaceous clay	Clay/claystone, iron-rich, organic-rich		
Jurassic	Jurassic sand/sandstone	Sand, silt and sandstone	Bagå Fm, Sorthat Fm, Hasle Fm, Rønne Fm	Michelsen *et al.* 2003
	Jurassic clay/ claystone	Clay and claystone		
Ordovician	Komstad limestone	Highly lithified micritic limestone with 5-20 % clay	Komstad limestone Fm	Buchardt & Nielsen 1985
Cambrian	Alum shale	Organic-rich shale	Læså Fm	Nielsen & Schovsbo 2007
	Broens Odde Member	Glauconitic siltstone and fine-grained sandstone		Buchardt & Nielsen 1985
	Balka Sandstone	Fine-to-medium grained quartzite, very little feldspar and clay matrix	Hardeberga Fm	
	Nexø Sandstone	Sandstone, 12-25 % feldspar, clayey	Nexø Fm	
Precambrian	Crystalline rock	Granite, gneiss		Waight *et al.* 2012

Fig. 2. Applied litho-chronological groups and related lithostratigraphical units for which this study provides thermal data. The colour code is applied throughout this paper. References to older works are found in the cited papers.

Recently, GEUS has acquired temperature logs in 13 boreholes, 150–300 m deep, mainly located in areas previously lacking temperature information. These areas were found as part of an initial compilation of data (Møller *et al*. 2014). Existing boreholes with indications of undisturbed temperature conditions were selected by querying the national geological and hydrological borehole database, Jupiter (Hansen & Pjetursson 2011). New temperature data were acquired using a conventional logging tool equipped with a thermistor-type probe and with continuous dense digital sampling.

So far, more than 1200 temperature logs from about 920 boreholes have been reported to the GERDA database. These logs were acquired as part of conventional well-logging suites for a variety of purposes (exploratory wells for groundwater mapping (Møller *et al.* 2009a), well-field investigations, and inspection of existing wells etc.), while other data were collected as part of specific high-precision temperature logging e.g. for groundwater flow investigations (e.g. Buckley *et al.* 2001). As most logs in this database were recorded shortly after drilling, these data are of highly varying quality. Logs, possibly without temperature disturbances (at least at the bottom), were selected by an automatic filtering routine using four criteria: Time of logging more than four days after drilling (cf. information in Nielsen *et al*. 1990); average temperature less than 14°C; logged depth interval larger than 50 m; and positive temperature gradients at depths greater than 50 m. All temperature logs satisfying these criteria were then visually inspected. Careful analysis led to the approval of 166 temperatures from the deepest parts of the wells (bottom hole temperatures of presumed minimum disturbances). Furthermore, 16 inflow temperatures at specific levels in open limestone/chalk wells with significant inflow of formation water were approved, and finally also eight full temperature logs of good quality, showing undisturbed conditions, were accepted. By these criteria data from more than 1000 temperature logs were discarded, mainly due to disturbance most likely from the drilling process or due to insufficient accuracy (e.g. lack of probe calibration and testing).

Thus, in this study, selected temperature logs from 56 boreholes covering the depth range 100–300 m were used (see list in Supplementary data file 1). These boreholes are distributed across most of the country in a variety of geological settings, see Fig. 1. In addition, 207 'local point temperatures' were accepted representing 180 borehole sites. These sites are less evenly distributed and show a significant clustering of sites in the north-eastern part of Sjælland (Fig. 1), where many open wells in limestone formations have been logged as part of different groundwater projects.

An example of a high-precision temperature log from a borehole at Harre in north-western Jylland (Fig. 1) is displayed in Fig. 3A. This borehole (DGU no 46.611) was drilled in 1980 to a depth of 285 m with continuous coring. The purpose was to perform a detailed analysis of the present shallow temperature and heat flow structure (Balling *et al.* 1981). As the penetrated layers are dominated by clay deposits, the risk of thermal disturbances from groundwater migration is believed to be minimal. Thus, this log contains the most detailed and accurate representation of thermal structure (temperature, temperature gradients, thermal conductivity and heat flow) for any shallow borehole within our study area and is therefore presented as illustration of the principal thermal features involved in our work. The continuous core was furthermore subjected to detailed lithostratigraphical and biostratigraphical studies (Nielsen 1994).

Thermal conductivity

As demonstrated by the data analysis below, thermal conductivity is the most important parameter in explaining both vertical and lateral variations in temperatures and temperature gradients.

The thermal conductivity of geological materials is controlled by mineral composition, texture, porosity and fluid content (e.g. Čermák & Rybach 1982; Brigaud & Vasseur 1989; Clauser & Huenges 1995). Furthermore, it depends on temperature and pressure (e.g. Robertson 1988; Clauser & Huenges 1995). Thermal conductivities of some main rock forming minerals, as well as of water and air, are listed in Table 1. Also included are information on density, specific heat capacity and thermal diffusivity. Combined with thermal conductivity, these parameters control transient thermal phenomena and are therefore applied in detailed numerical subsurface thermal modelling, including modelling of heat extraction and heat storage. Since quartz is a very common mineral and has a substantially higher conductivity than most other common minerals (Table 1), it is evident that the content of quartz is a major parameter controlling the overall conductivity of geological materials. In the shallow subsurface, pore spaces are normally filled with water with a low thermal conductivity or above the water table with air of very low conductivity. Thus, the porosity of the geological materials is a very important factor as well.

However, structure and texture, which are partly related to porosity and mineral content, may also affect the thermal conductivity (e.g. Davis *et al*. 2007). This is clearly illustrated for laminated clay deposits, which may show significant conductivity anisotropy with the highest conductivity in the direction parallel to lamination/bedding and the lowest conductivity in the perpendicular direction. Differences (anisotropy factors) of up to around two are reported (Balling *et al.*

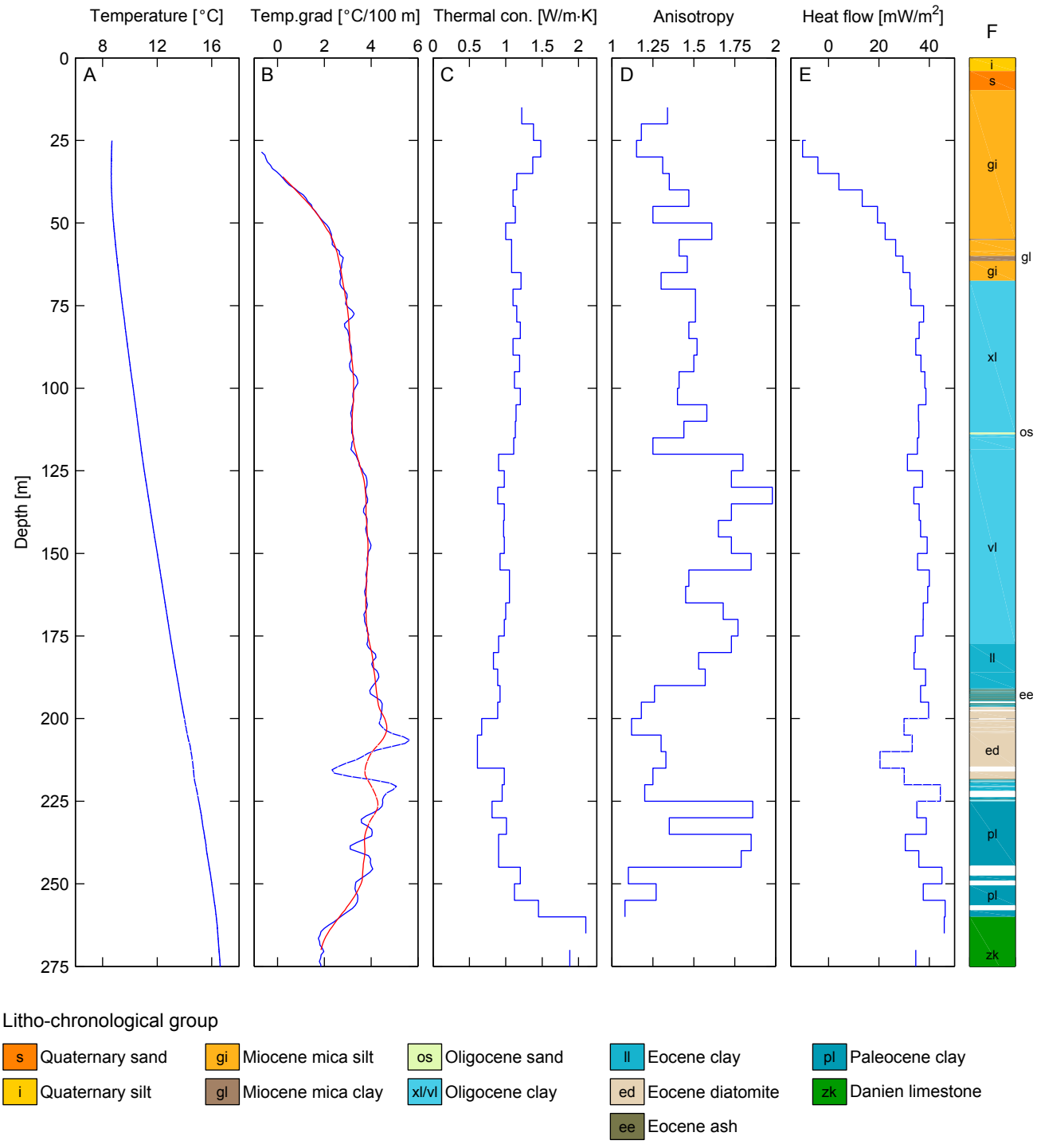

Fig. 3. Borehole at Harre, north-western Jylland (DGU no 46.611), illustrating detailed thermal information. **A:** temperature log (measured 2012). **B:** interval temperature gradients (5 m: blue; 20 m: red, running mean). **C:** thermal conductivity (vertical component). **D:** factor of conductivity anisotropy (ratio of horizontal to vertical component). **E:** heat flow. **F:** lithological log; white intervals: no core. Conductivity and heat flow shown as mean values for 5 m intervals. Borehole information and conductivity data from Balling et al. (1981). Even though the temperature log was measured 32 years after drilling, locally at 200–225 m temperatures and related temperature gradients and heat flow have not yet reached thermal equilibrium (dashed lines in A, B and D). This is known to be related to a local cavity developed in the soft diatomite during drilling and subsequently cemented along with cementing iron tubing for temperature logging. Heat from the cemented cavity has not fully dissipated.

1981; Čermák & Rybach 1982; Robertson 1988; Davis *et al*. 2007). Depending on which laboratory equipment is applied, the two perpendicular components may be measured (c.f. Balling *et al*. 1981; Davis *et al*. 2007).

Thermal conductivity is also dependent on ambient temperature and pressure conditions. Conductivity increases with increasing pressure and, for most lithologies, conductivity decreases with increasing temperature (e.g. Robertson 1988; Somerton 1992; Clauser & Huenges 1995). However, for depth and temperature intervals considered in this study, effects are small, as thermal conductivities were measured at temperatures close to *in situ* conditions. Only for pressure, an effect was considered. An increase of conductivity by up to 5–10% is observed at relatively low pressures of 5–10 MPa, equivalent to depths of about 250–500 m (Balling *et al*. 1981; Clauser & Huenges 1995). This increase at relatively shallow depth is mainly due to the closing of pores and micro cracks and due to better thermal contact between the individual mineral grains. However, limited knowledge about the detailed behaviour of this low-pressure change in thermal conductivity is available. Especially for sediments with high porosity, more studies are needed. In the present data sets, laboratory conductivity was corrected, generally by +5%, to approximate *in situ* conditions when used for heat flow determination (Balling 1986).

Our thermal conductivity data originate from recent laboratory measurements on sediment samples, largely from well-characterised outcrops and a few boreholes (Pagola 2013; Ditlefsen & Sørensen 2014), and from a compilation of previously published measurements, mainly from core materials and some outcrops (e.g. Balling *et al*. 1981, 1992; Kristiansen *et al*. 1982).

During 2011–2013, Ditlefsen & Sørensen (2014) collected a total of 59 samples representing 11 litho-chronological groups for thermal conductivity measurements at 15 localities, primarily in eastern Jylland (Fig. 1). The consolidated sediments were sampled directly in tubes to obtain undisturbed samples (diameter of 7.5 cm or 10 cm and a length of 20 cm), while loose sediments were sampled in plastic bags and vibrated into sample holders in the laboratory.

Over the years from the late 1970s to the early 1990s, the older thermal conductivity data were measured on core material from 19 boreholes covering Maastrichtian chalk, Palaeogene limestone and clay, Neogene clay and sand deposits, Quaternary marine clay as well as shallow Jurassic deposits on Bornholm (Fig. 1). Not all individual measurements, which amount to several hundred values, were available. For shallow cored boreholes, most results were presented as mean conductivity over specified depth intervals, often of 5 m (as in Fig. 3C) or 25–50 m length. Such 5 m interval mean values were digitised from graphs. Furthermore, some values from Bornholm originate from cylindrical probe *in situ* measurements (Kristiansen *et al*. 1982). This applies to 11 locations with Precambrian crystalline rocks and six locations with Palaeozoic sedimentary rocks. All measurements are listed in Supplementary data file 2.

All new, and most old data, were measured using the classic needle-probe technique, which is a transient

Table 1. Thermal properties and density of common rock-forming minerals, air and water at standard laboratory conditions

Material	Thermal Conductivity W/(m·K)	Density kg/m^3	Specific heat capacity J/(kg·K)	Volumetric heat capacity MJ/(K·m^3)	Thermal diffusivity 10^{-6} m^2/s
Quartz-a	7.69[a]	2647[a]	740[d]	1.959	3.92
K-feldspar	2.45[a]	2565[a]	700[d]	1.796	1.36
Plagioclase	1.78[a]	2688[a]	837[d]	2.250	0.79
Muscovite	2.32[a]	2852[a]	760[d]	2.168	1.07
Biotite	2.02[a]	2981[a]	770[d]	2.295	0.88
Glauconite	1.63[a]	2848[a]			
Hornblende	2.81[a]	3183[a]			
Calcite	3.59[a]	2721[a]	815[d]	2.218	1.62
Smectite	1.88[b]	2630[b]			
Illite	1.85[b]	2660[b]			
Kaolinite	2.64[b]	2630[b]	930[d]	2.446	1.08
Chlorite	5.14[a]	2755[a]	600[d]	1.653	3.11
Halite	6.50[c]	2163	916[d]	1.981	3.28
Water	0.60	1000	4186[d]	4.186	0.14
Air	0.026	1.225	1005[d]	0.001231	21.1

Calculated values for volumetric heat capacity (product of specific heat capacity and density) and thermal diffusivity (ratio of thermal conductivity and volumetric heat capacity).

[a]Horai (1971). [b]Brigaud & Vasseur (1989). [c]Clauser & Huenges (1995). [d]Waples & Waples (2004).

method based on the theory of temperature propagation from a linear source (Von Herzen & Maxwell 1959; Kristiansen 1982; Bording *et al.* 2019). All laboratory measurements represent values for water-saturated conditions and laboratory ambient temperature (*c.* 20°C) and pressure (0.1 MPa = 1 bar).

To investigate the characteristic thermal conductivities for lithological units of similar mineralogical and textural composition, data were grouped according to a litho-chronological classification (Fig. 2). However, determining a characteristic mean thermal conductivity for such a group is not straightforward. Data density varies from single sample measurements to mean values of several densely spaced core measurements covering intervals between 5 m and 50 m, e.g. Fig. 3.

In order to ensure that localities with closely spaced measurements do not dominate within a litho-chronological group, the mean thermal conductivity of a group was calculated based on 'locality' mean thermal conductivities. If measurements within a specific litho-chronological group represent a cored depth interval of more than 50 m, each 50 m interval counts equivalent to 'a locality'. Due to the inhomogeneous data set, a meaningful conductivity standard deviation related to mean values may not be calculated. Instead, the range of 'site mean values' is given (Appendix A).

Since the quartz content is one of the major factors controlling the thermal conductivity, this content was determined together with the thermal conductivity of a number of samples collected recently at outcrops. The quartz content was determined at Aarhus University by X-ray diffractometry (XRD) on pulverised samples.

Thermal diffusivity

Very little information is available on laboratory measurements of rock thermal diffusivity, the parameter controlling transient thermal phenomena. Kristiansen (1982) published a 75 m section of Oligocene clay from the Harre borehole with densely spaced needle-probe results. Measured values are within the approximate range of (0.4–0.8) × 10^{-6} m^2/s. Here, similar to thermal conductivity (Fig. 3), thermal diffusivity shows significant thermal anisotropy with the horizontal component larger than the vertical component. When information on thermal diffusivity is needed, this parameter may typically be calculated (according to its definition), from the ratio of thermal conductivity to volumetric heat capacity (cf. Table 1).

Lithological information

Lithological information was extracted from all boreholes with undisturbed temperature logs. The main source for borehole lithological information was the Danish national geological and hydrological borehole database Jupiter, to which lithological sample descriptions are reported. Here sample materials are described and interpreted by geologists following standards outlined by Gravesen & Fredericia (1984), including interpretation of depositional environment, chronostratigraphy and, when possible, also lithostratigraphy. For a few research and deep boreholes, the lithological information was found in scientific publications and well completion reports. Sources of lithological information are listed in Supplementary data file 1 and linked to the Jupiter database where possible. Figure 3F illustrates a litho-chronological log for the geological settings in clay-rich Neogene and Palaeogene sequences of the Harre borehole.

Temperature gradient

Interval temperature gradients were calculated using a linear least-squares approach, with a gradient fitted to all temperature data from within 5 m or 20 m depth intervals. Interval gradients were determined for every 2.5 m from the continuous logs and at the sampling point for the discrete logs. In order to reduce uncertainties related to different sampling positions, the 20 m interval temperature gradients were used for the present lithological correlation analysis, despite the fact that the 5 m interval gradients depict more detailed lithological variations (e.g. Fig. 3B).

Temperature gradient – lithology relation

The 20 m interval temperature gradients were assigned to specific litho-chronological groups (Fig. 2) based on the lithological sample descriptions of the interval. A temperature gradient value was only assigned to a specific litho-chronological group if at least 90 per cent of the 20 m section is related to the lithology in question.

When calculating mean values and standard deviation of temperature gradients for each litho-chronological group, as well as when plotting histograms or bar plots, it has to be ensured that there is not an inappropriate dominance from boreholes with thick sequences of the same lithology. This was achieved by assigning a weight factor to each temperature gradient value belonging to a particular litho-chronological group. As for the thermal conductivity data, litho-chronological groups of up to 50 m thickness within a given borehole counts as 'only one locality' (each temperature gradient value, calculated with a 2.5 m depth interval, is weighted with the reciprocal of the number of observed temperature gradients belonging to the same litho-chronological group within a

50 m depth section). This procedure was applied for calculating weighted mean values of temperature gradients with standard deviation (expressed as one standard deviation) as well as for the temperature gradient bar plots.

Estimation of heat flow

The determination of the flow of heat (Q) from the Earth's interior to its surface is based on Fourier's law of heat conduction,

$$Q = k \frac{dT}{dz} \quad (1)$$

where k is thermal conductivity, T the temperature, and z the depth.

Classically, local site values of heat flow are determined from measured temperature gradients in sections of a borehole, in combination with information on thermal conductivity from the same interval, preferably from laboratory core measurements (Powell *et al.* 1988). The heat-flow depth profile of the Harre borehole (Fig. 3E) is determined in this way. An alternative procedure is the so-called Bullard method (Bullard 1939; Powell *et al.* 1988), by which heat flow in a borehole is determined from the slope of a correlation line observed when plotting the temperature-depth function against thermal resistance (depth increments divided by thermal conductivity).

A somewhat similar procedure may be applied to our data set. If heat flow is almost constant, or does not vary much within a specific region, it follows from Eq. (1), that the temperature gradient and the reciprocal of thermal conductivity are (approximately) linearly related and the heat flow is given by the slope of the regression line. Thus, heat flow may be estimated by defining the least squares linear regression line from a set of data combining characteristic mean temperature gradients and mean thermal conductivities for associated lithologies. This procedure may be applied to a conductive regime of insignificant heat production for the depth intervals in question. We applied this methodology to our dataset and obtained a characteristic near surface heat-flow estimate for onshore Denmark. For lithologies known to show thermal conductivity anisotropy, only data representing the vertical component of the conductivity were used.

When applying the least squares procedure of York *et al.* (2004) for estimating the slope (heat flow) and intercept of the correlation line with uncertainties, error bars on both observation parameters, reciprocal thermal conductivity and temperature gradients, are required. For temperature gradients, the calculated standard deviations (Appendix B) were used except for few data points with very low values originating from only few observations. Here standard deviations were estimated from those of neighbouring units. As discussed above, standard deviations for mean thermal conductivities were not calculated due to the different nature of data. Here, based on measurements from outcrop samples, a uniform uncertainty estimate of 15% was applied.

Results

Temperature field

As outlined above, our temperature dataset consists of 56 detailed borehole temperature logs, and 207 local point measurements mainly from bottom-hole temperatures and 'local water-inflow temperatures'. Furthermore, we include a series of repeated measurements from one borehole site representing the depth penetration of the annual surface temperature wave.

Over a time period of one year (March 1982 to February 1983), a series of 10 temperature–depth data (one metre step for the depth interval 1–25 m) were measured in a borehole at Jebjerg (Fig. 4). This data set clearly illustrates the depth penetration of the annual surface temperature wave. The measurements display temperature differences by about ± 5°C at a

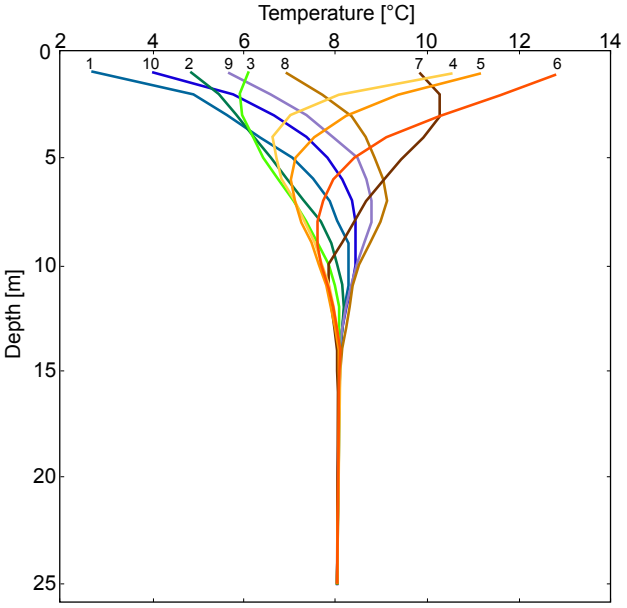

Fig. 4. Depth penetration of the annual surface temperature variation as measured in a borehole at Jebjerg, north-western Jylland (DGU no 46.594; see also Fig. 1). Data measured during the period of March 1982 to February 1983 by the geophysics group, Aarhus University (Knudsen 1983). Numbers indicate time of measurement: 1, primo March; 2, medio April; 3, medio May; 4, medio June; 5, primo July; 6, ultimo August; 7, primo November; 8, ultimo December; 9, medio January; 10 ultimo February.

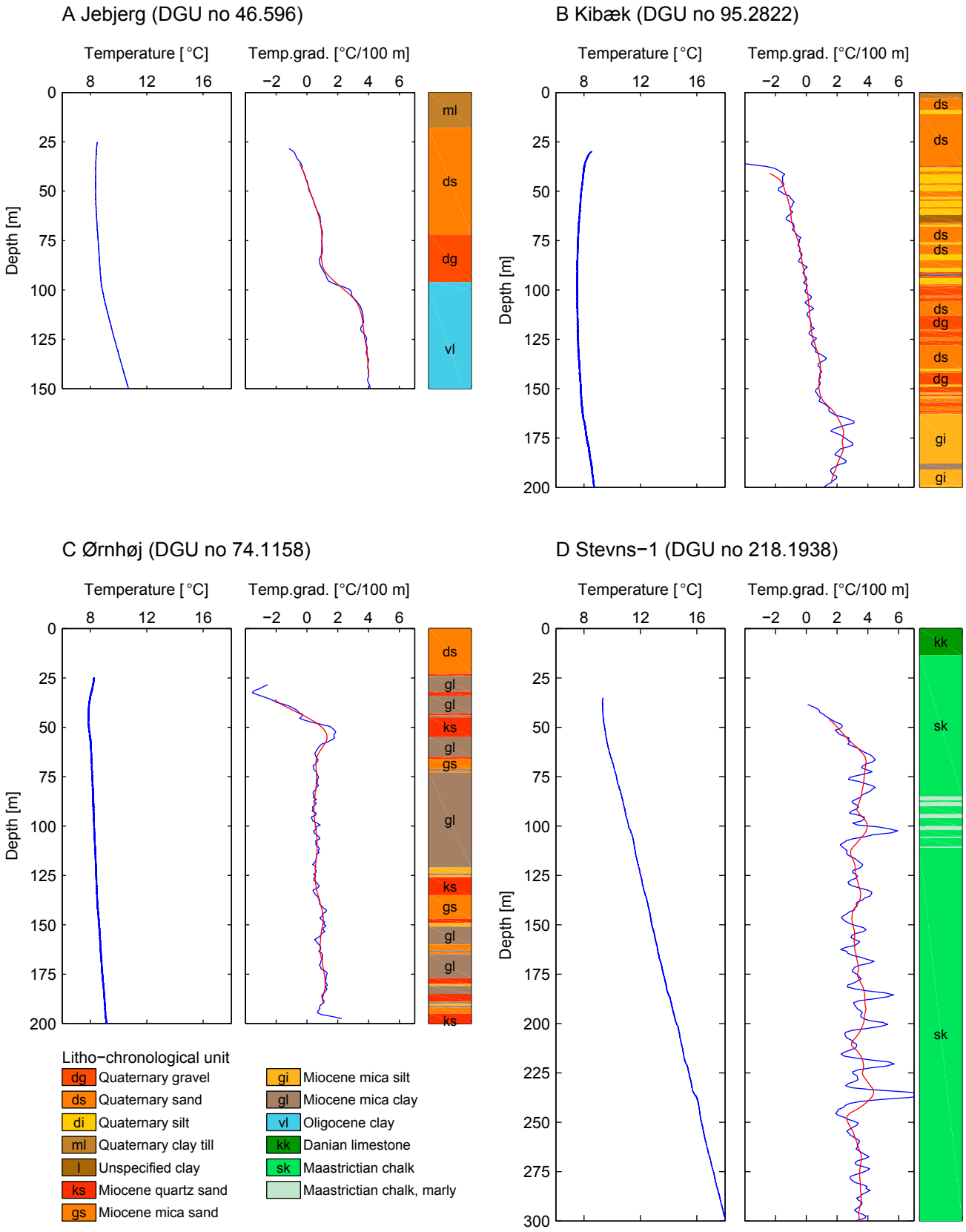

Fig. 5. Selected examples of detailed borehole temperature information. Measurements from 2007 to 2013. Temperature gradients are displayed as running mean values of 5 m (blue) and 20 m (red) intervals. Locations are shown in Fig. 1. See text for description.

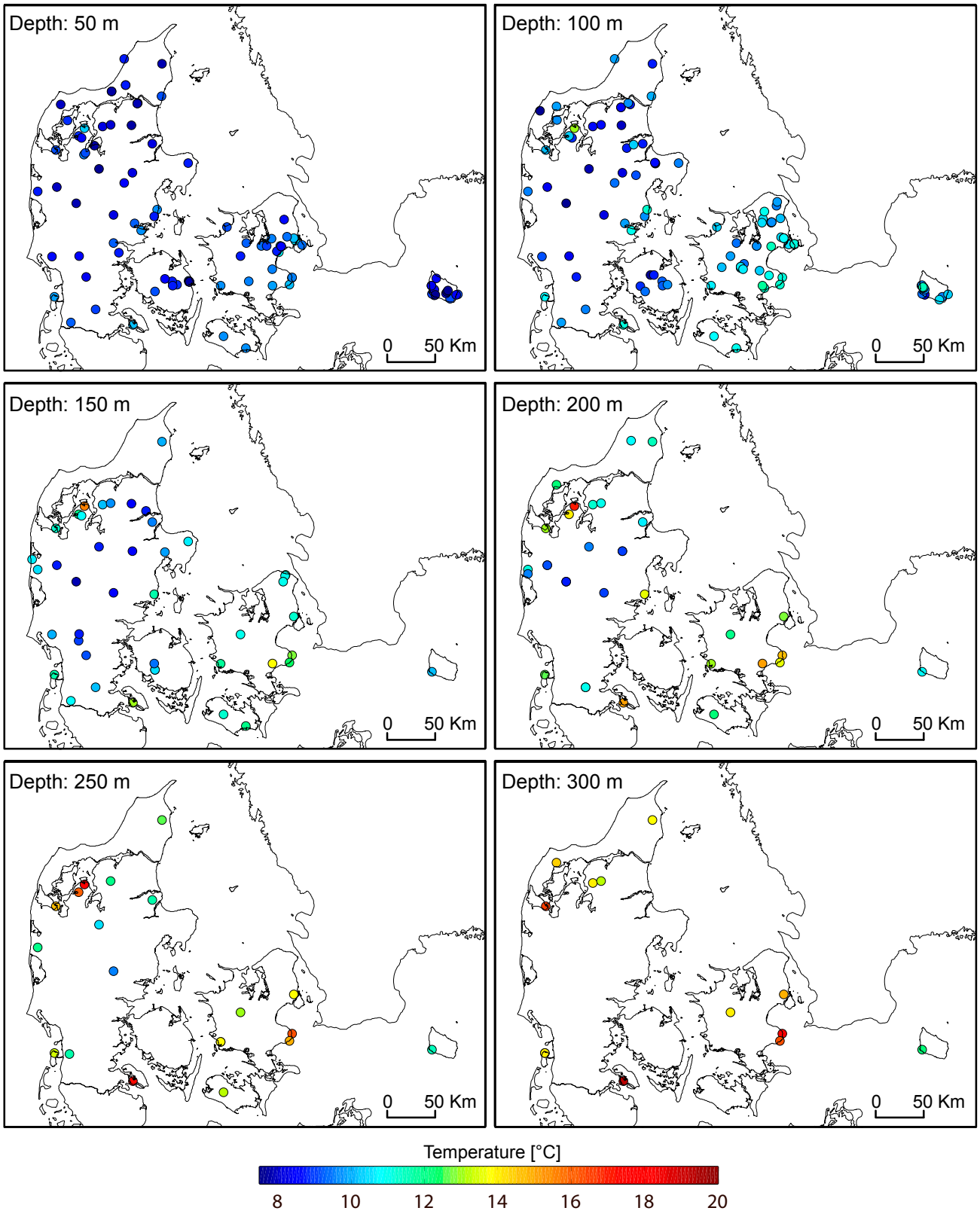

Fig. 6. Measured borehole equilibrium temperatures for selected depths (metres below ground level).

depth of 1 m, about ± 1.5°C at a depth of 5 m and less than 0.1°C below 15 m depth. The amplitude of the penetrating annual surface wave depends on local thermal conditions as well as variations in weather conditions; observations at different boreholes over two time periods show that at 5 m depth, these yearly temperature differences can vary *c.* 0.5°C (Knudsen 1983; Møller *et al.* 2014).

Figure 5 shows, for illustration, selected examples of borehole temperature logs and the calculated temperature gradients at different geological settings and geographical locations (Fig. 1). All four boreholes show very low, or even negative, temperature gradients in the shallowest parts. These selected boreholes also illustrate that temperatures at 200 m depth vary by several degrees.

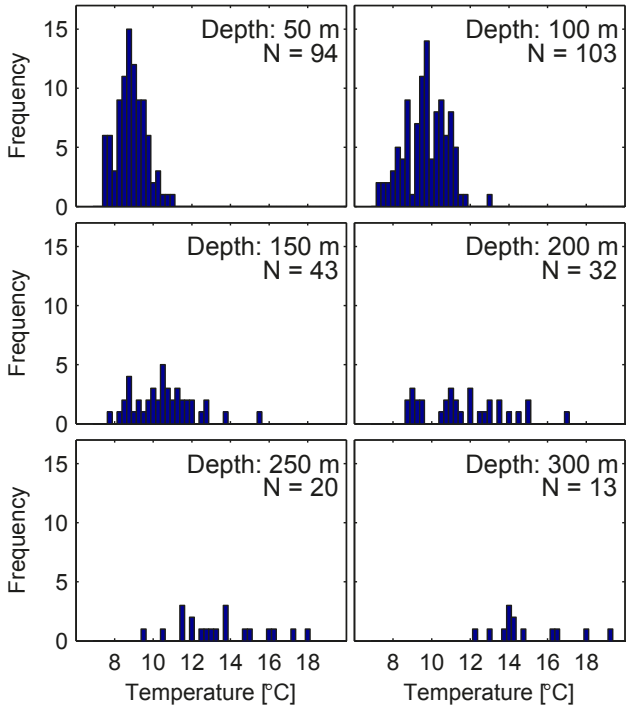

Fig. 7. Histograms of measured borehole temperature for selected depths as indicated. Same data as displayed in Fig. 6 and Table 2.

Table 2. Temperature distribution with statistical information from selected depths

Depth m	N	Mean °C	Std. dev. °C	Median °C	Min. °C	Max. °C
50	94	8.9	0.8	8.8	7.4	11.0
75	132	9.2	0.9	9.3	6.7	11.6
100	103	9.7	1.1	9.7	7.3	13.0
150	43	10.5	1.6	10.6	7.8	15.5
200	32	11.6	2.2	11.2	8.7	17.1
250	20	13.4	2.2	13.2	9.6	17.9
300	13	14.9	2.0	14.2	12.2	19.3

Depth: metres below ground level.
N: number of temperature data at the indicated depth.
The median value is not significantly different from mean value.
The range of temperatures at specific depths is indicated by the measured minimum and maximum values.

Temperature-field data from selected constant depths between 50 and 300 m are displayed in Fig. 6 and summary statistics are given in Fig. 7 and Table 2. If densely sampled logs were not available, data were included from within depth intervals of up to ± 12.5 m from reference depth. For typical temperature gradients of 1–3°C/100 m, an up to 12.5 m depth shift may thus result in a temperature bias within the range of ± 0.13 to ± 0.38°C.

Except for the upper part of the boreholes, mean temperatures generally increase with depth as shown in Fig. 5. At 50 m depth, the mean value of 8.9 ± 0.8°C (one standard deviation) has increased only little compared to the mean annual ground temperature (see section discussions). The higher mean values at 100 and 200 m of 9.7 ± 1.1°C and 11.6 ± 2.2°C, respectively, reflect this general increase. Furthermore, we observe a marked increase in standard deviation with increasing depth, consistent with a significantly increasing temperature range with increasing depth (cf. Fig. 7). At 100 m the observed range of temperatures is 7.3–13.0°C while it is 8.7–17.1°C at 200 m. The standard deviation on mean temperature at 250 m is almost three times larger than that at 50 m (Table 2). From our maximum depth of 300 m, data from only 13 borehole sites are available, however, still presenting valuable information, both locally and by showing a significant range of temperatures (12.2–19.3°C; mean value 14.9°C).

These deeper levels clearly show significant and systematic lateral temperature variations across the country. The higher temperatures are observed in the eastern and southern part of Sjælland, on the island of Lolland and in parts of north-western and eastern Jylland, while lower temperatures are found in central Jylland and on parts of Bornholm.

Thermal conductivity

Information on thermal conductivity of the applied litho-chronological groups (Fig. 2) is displayed in Fig. 8. Details are found in Appendix A. Thermal conductivities of the investigated lithologies, commonly present at shallow depths, cover the range 0.6–6 W/(m·K) with the majority of values between 1 and 3 W/(m·K). The content of water of low conductivity (related to porosity) and the amount of quartz of high conductivity (Table 1) are the two main factors controlling the bulk thermal conductivity.

To illustrate the importance of the quartz content on thermal conductivity, this content was determined in 12 samples of different lithologies (Fig. 9). As expected,

Fig. 8. Thermal conductivities for litho-chronological groups with decreasing stratigraphic age upwards. Crosses indicate mean values and colour bars show the range of measured conductivities. Colour code as in Fig. 2.

a general increase in thermal conductivity is observed for increasing quartz content, although some scatter is present. A variation of 20–30% in quartz content for samples with similar thermal conductivity is seen, with the sandy samples having the highest quartz content and the clay-rich samples the lowest quartz content. Although not measured, the sandy samples are likely to have the highest porosity (content of water of low conductivity), resulting in their reduced thermal conductivity compared to the clay-rich samples.

Lowest conductivities, with a mean value of about 0.6 W/(m·K), are observed for the organic-rich Quaternary gytja and porous Eocene diatomite. The very fine-grained Eocene and Paleocene clay deposits also have very low mean thermal conductivities, around 1.0 W/(m·K). With increasing content of silt and fine sand, the examined clay deposits show an increasing conductivity. This is seen in the slightly silty Oligocene clay with a mean conductivity of 1.15 W/(m·K), in the silty and sandy Jurassic clay, the silty Miocene Mica clay, and the silty Quaternary marine clay, all with mean values of around 1.3 W/(m·K). A higher mean value is also observed in Quaternary meltwater clay (1.6 W/(m·K)), but with a relatively large scatter on data from different locations. Furthermore, Quaternary clay till have relatively high conductivities of around 2.0 W/(m·K), which is probably because they contain fractions of sand and gravel dominated by quartz. Thus, the conductivity of shallow clay deposits may vary with up to a factor of two, which emphasises the relevance

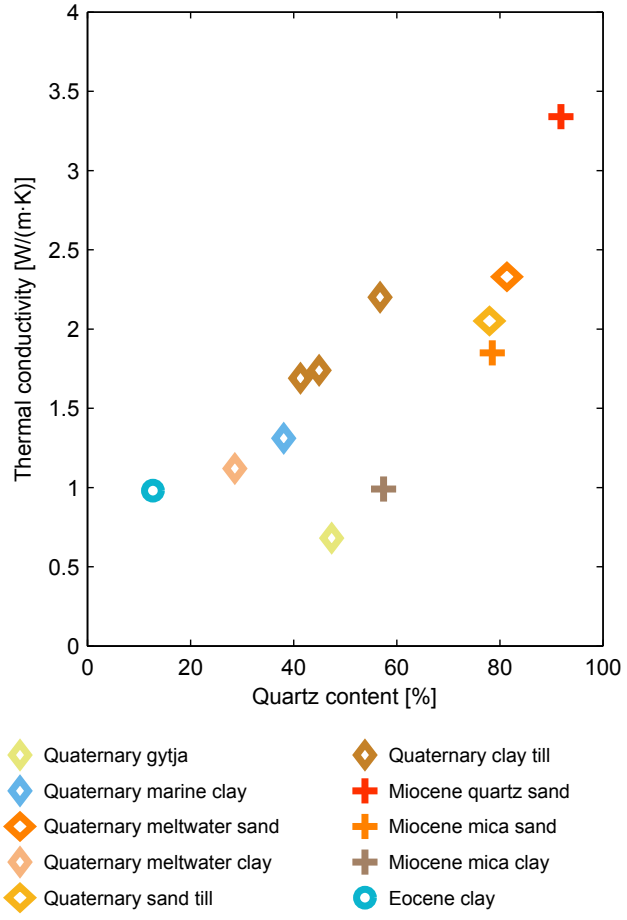

Fig. 9. Thermal conductivity versus quartz content determined on selected lithologies. Colour code as in Fig. 2.

of dividing clays into litho-chronological groups.

The Danian limestone and the Maastrichtian chalk show intermediate mean conductivities, around 1.4 and 1.7 W/(m·K), respectively. This difference is in good agreement with an expected higher porosity of the Danian Limestone compared with the Maastrichtian chalk.

Values of around 1.8 to 2.2 W/(m·K) are found for fine-grained sand deposits and sand deposits with a substantial silt and clay fraction, e.g. Quaternary sand tills, silty and fine-grained Quaternary marine sand and Miocene mica sand. Higher conductivities, with mean values of 2.3–2.6 W/(m·K), are found in a number of sand deposits including Quaternary meltwater sand, Miocene quartz sand and Jurassic sand and sandstone.

The highest thermal conductivities are measured in Palaeozoic sandstones from Bornholm with a high content of quartz and low porosity. The Cambrian Balka sandstone, consisting of almost pure quartz, has a mean thermal conductivity of 6.1 W/(m·K). Relatively high values are also found in the Nexø Sandstone (4.1 W/(m·K)), containing both quartz and feldspar, and in the Cambrian Broen Odde Member, a fine-grained glauconitic greenschist sandstone with silt beds, with a mean conductivity of 4.1 W/(m·K).

Precambrian granites and granitic gneiss with quartz contents in the range 22–33% have a mean thermal conductivity of 3.1 W/(m·K), which is typical for those rock types (Robertson 1988; Clauser & Huenges 1995). The Ordovician Komstad limestone has a mean conductivity of 2.7 W/(m·K), which is significantly higher than that of the Danian Limestone and the Maastrichtian chalk, probably due to a low porosity compared to the younger limestone formations. Cambrian Alum shale has a mean conductivity of 1.7 W/(m·K), the lowest value found among the Palaeozoic rocks of low porosity. This is due to a low quartz content and a relatively high content of organic material.

Relation between temperature gradients and lithologies

Detailed information on temperature gradients, represented as 20 m interval mean values, are displayed in Fig. 10 and Fig. 11 as well as in Appendix B. Data originate from the 56 boreholes that provide accurate equilibrium temperature logs. In these figures, the temperature gradients are shown in relation to the litho-chronological units over which they are calculated, and they are divided into two classes according to depth, 50–100 m and > 100 m. At depths shallower than 100 m, temperature gradients are generally perturbed by the depth penetration of the recent increase in mean annual surface temperature (Møller *et al.* 2014). Within the uppermost 50–100 m, even negative temperature gradients (decreasing temperatures with depths) are observed (Fig. 5).

For the depth interval 50–100 m, gradients between c. -2 and +5°C/100 m are observed. Below 100 m the gradients range between values close to zero and 5°C/100 m, thus, still locally, very low values are observed, but no negative gradients. For the depth interval 50–100 m, the temperature gradients show a very high degree of scatter within the litho-chronological groups, while for the deeper levels gradients to a large degree show a narrower range for each litho-chronological group, though with partly or completely overlap between groups.

For depths below 100 m the mean temperature gradient for the various litho-chronological groups overall show an inverse correlation to the mean thermal conductivity in accordance with Eq. (1). Thus, coarse-grained, quartz-rich sediments show low mean temperature gradients (*c.* 0.8–1.2°C/100 m), the silty clay groups and the limestone and chalk groups have intermediate gradients (*c.* 1.6–2.5°C/100 m) and the very fine-grained clays have high temperature

gradients (*c*. 3.3–4.3°C/100 m).

Heat flow

At the Harre borehole, local site values of heat flow (Fig. 3E) were determined from temperature gradients calculated over 5 m intervals and vertical thermal conductivities from the same intervals. The average heat flow from undisturbed sections of the borehole (75–200 m, 225–275 m) is 37.3 ± 3.5 mW/m². Conductivity was measured with close sampling along the cores shortly after drilling (to ensure an intact water content) and detailed resolution of conductivity anisotropy (Balling *et al*. 1981), thus resulting in a well-defined local-site

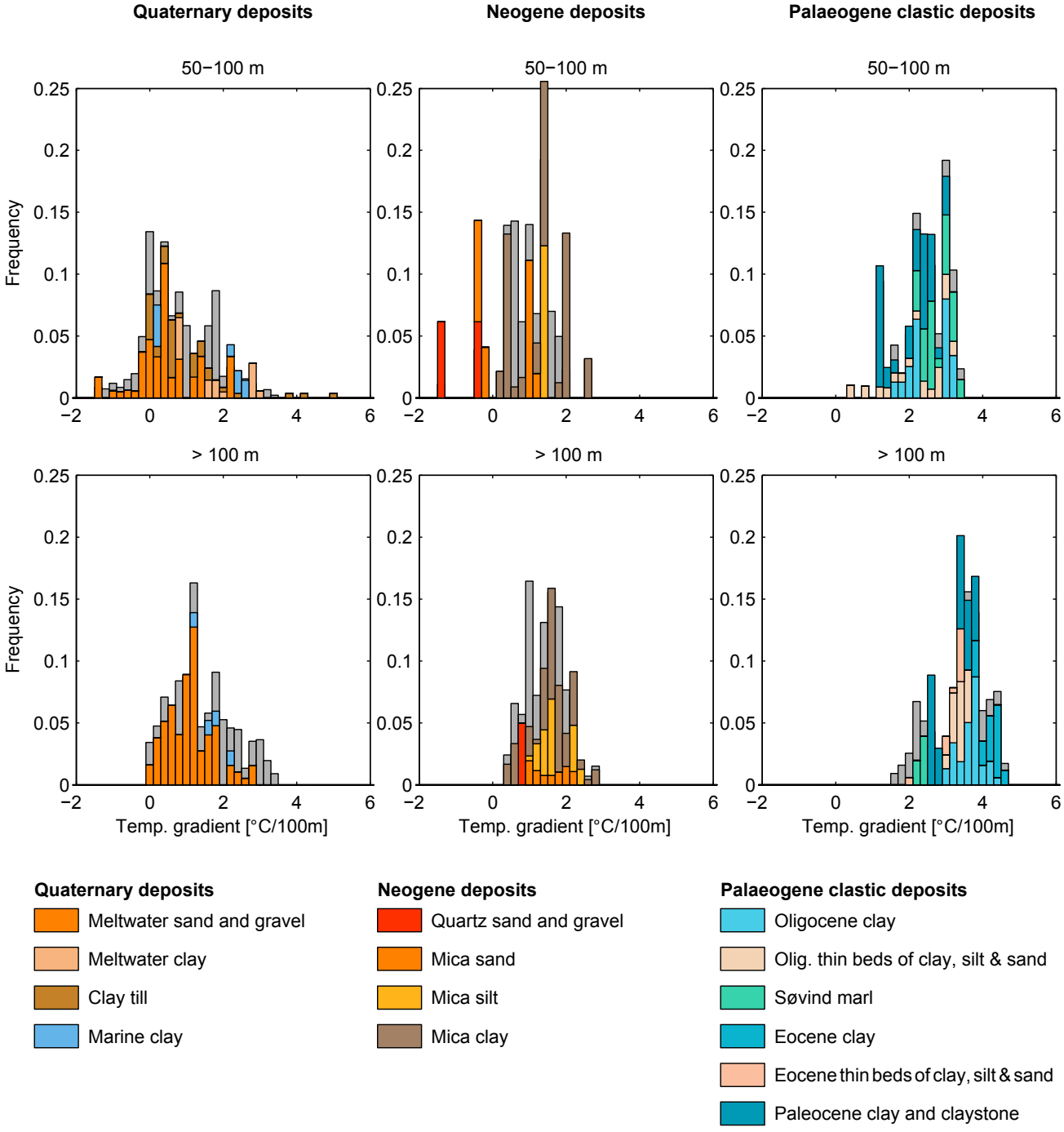

Fig. 10. Temperature gradients, displayed as bar plots, for two depth intervals measured in Quaternary, Neogene and Palaeogene clastic deposits. The grey bars, displayed behind the coloured bars, represent the temperature gradient distribution of all data, not divided into litho-chronological groups, within Quaternary, Neogene and Palaeogene deposits, respectively.

shallow heat-flow estimate.

As discussed above in relation to equation (1), the characteristic heat flow for a certain area may be obtained from the regression line in a plot of mean temperature gradients against the reciprocal of mean thermal conductivity. For our data set, with combined information on mean temperature gradients and thermal conductivity for litho-chronological groups, these parameters are plotted in Fig. 12. Only data from depths greater than 100 m are included, except for the Cambrian and Precambrian data from Bornholm measured around 1980. For clays (Jurassic clay, Oligocene, Eocene and Paleocene clays, Miocene mica clay, Miocene mica silt and silty Quaternary marine clay), expected to have significant thermal conductivity anisotropy, the vertical component data are applied. The mean thermal conductivity may thus be lower than the mean values displayed in Fig. 8 and Appendix A.

Since it is well known that drilling mud may take up fine sand and silt fractions from the sediments, leaving

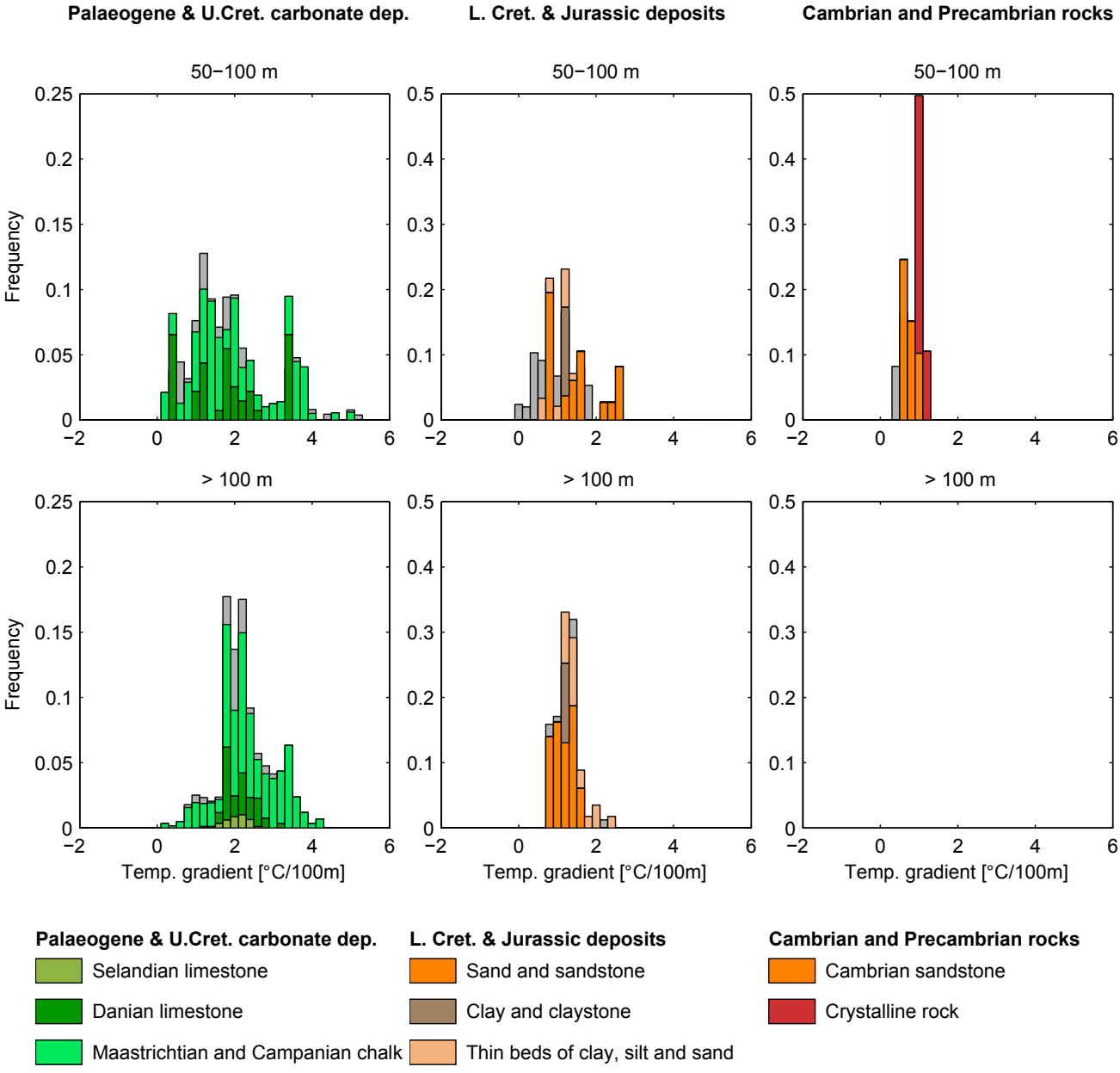

Fig. 11. Temperature gradients for two depth intervals measured in Palaeogene and Upper Cretaceous carbonates, Lower Cretaceous and Jurassic deposits and Cambrian and Precambrian rocks. The grey bars, displayed behind the coloured bars, represent the temperature gradient distribution of all data, not divided into litho-chronological groups, within Palaeogene and Upper Cretaceous carbonates, Lower Cretaceous and Jurassic deposits and Cambrian and Precambrian rocks, respectively.

mostly clay cuttings for description, borehole samples described as silty clay may potentially originate from sediments with a higher content of silt and fine-grained sand. Therefore, data from silty clays and silt (Quaternary marine clay, Miocene mica silt and clay) in this context are treated as outliers with too low temperature gradients and are not included as data points.

The least squares regression line in Fig. 12 yields a heat flow estimate of 37 ± 5 mW/m² and an intercept value of 0.0 ± 0.2°C/100m. The fact that the best-estimate relation intersects the origin, with small uncertainty limits, supports the notion of an unbiased well-defined regional estimate of shallow-depth heat flow.

Discussion

Through compilation and analysis of all available information on measured borehole temperatures and rock thermal conductivity measurements from depths up to about 300 m, we outline regionally representative quantitative information on the shallow subsurface thermal structure for onshore Denmark.

Temperatures

In order to avoid disturbed temperature measurements our analysis focuses on temperature data collected at depths more than 50 m below the surface. The largest number of temperature measurements of sufficient quality is available for the depth range 75–100 m (Table 2). With increasing depth, the number of data decreases, however highly valuable information is available also for the deeper levels of 200–300 m.

At a depth of 50 m a mean temperature of 8.9°C is found (range 7.4–11.0°C), which is close to the mean annual ground surface temperature as reported by the Danish Meteorological Institute (7.7°C weather normal of 1961–1990 (DMI 2018a) and 8.8°C decadal mean of 2001–2010 (DMI 2018b)). Regional and local variations of mean surface values of *c*. 1.5°C are observed (Scharling 2012). Local variations of the mean annual ground surface temperatures, at site level, have also previously been obtained from our dataset by 'extrapolating borehole temperatures to surface intercept' of shallow temperature logs. Variations of up to 3°C (range of values 7–10°C) were found. These differences are believed to be related to variations in surface environmental conditions such as open land, forest, city, northern and southern slopes etc. (Møller *et al*. 2014).

With increasing depth, temperature variations across the country increases markedly (Figs. 6–7). Thus, in contrast to often-held assumptions, the data clearly demonstrate the existence of significant temperature variations at relatively shallow depths. For instance, we note that the observed lowest temperatures at depths of 200 and 250 m (8.7 and 9.6° C, respectively) are at the same level as characteristic mean temperatures at depths of 50–100 m, and they are clearly lower than the highest temperatures at these depths (Fig. 7). The temperature variations as displayed in Fig. 6 are further discussed below.

Thermal conductivities

Some samples, in particular laminated clays, show

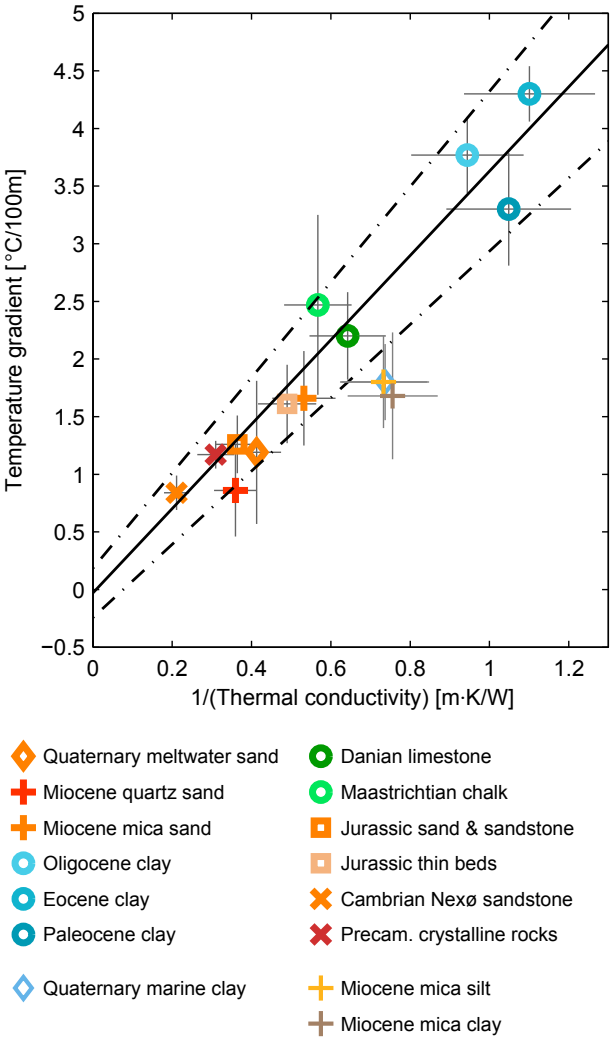

Fig. 12. Mean temperature gradients versus 1/(mean thermal conductivity) for lithologies of combined parameter information. Uncertainty estimates are indicated for both parameters. From the slope of the least-squares regression line (full line), heat flow is estimated at 37 ± 5 mW/m² and the estimate for intercept is 0.0 ± 0.2°C/100m. Dashed lines indicate uncertainty limits (one standard deviation). Quaternary marine clay and Miocene mica silt and clay are treated as outliers and are not included in the regression.

significant anisotropy in thermal conductivity. Conductivity parallel with lamination/bedding (normally the horizontal component of conductivity) is generally higher than perpendicular to lamination/bedding (normally the vertical component) (Balling *et al.* 1981; Brigaud & Vasseur 1989; Davis *et al.* 2007). In the Harre borehole (Fig. 3) we see significant conductivity anisotropy in most lithologies, and anisotropy factors (ratio between the horizontal and the vertical component of conductivity) up to 1.5–1.8. This is regarded as typical for clay deposits and other laminated rocks. Here, the thermal conductivity may not be characterised by just one number for all purposes and it is important that two perpendicular components are measured.

For the determination of heat flow and understanding of temperature gradient variations, information about the vertical conductivity is needed. However, for thermal modelling of heat extraction and storage in conductive systems of vertical boreholes (BTES, Hellström 2011), the horizontal conductivity is relevant as well. For modelling systems of aquifer thermal energy storage (ATES, Andersson 2007), the vertical component of conductivity of layers above and below the aquifer is also important.

Heat flow

An estimate of the shallow regional heat flow of 37 ± 5 mW/m^2 has been made based on information on mean temperature gradients (below 100 m depth) and mean thermal conductivities of the main litho-chronological groups (Fig. 12). The value is (coincidentally) identical with that determined for the Harre borehole (Fig. 3) using classical techniques. Such a low level of heat flow is also fully consistent with shallow heat-flow observations from a number of boreholes presented in Balling (1986) and Balling *et al.* (1981, 1992), see also the recent analysis in Balling (2013). Since this shallow heat flow is much lower than the mean deep background heat flow of around 70–75 mW/m^2 found in the Danish area (Balling 1992, 2013), an explanation is needed. The difference is interpreted as due to long-term palaeoclimatic effects mainly caused by a 'slow subsurface penetration' of the temperature rise associated with the termination of the last glaciation (Kukkonen & Jõeleht 2003; Balling 2013). Any numerical subsurface temperature modelling applies information on thermal boundary conditions in terms of temperatures and/or heat flow. For shallow thermal modelling, it is important that the observed low level of heat flow is applied instead of up to twice the value observed for the deep background heat flow or standard values (about 65 mW/m^2) for continental heat flow.

Even though a significant scatter is seen in the relationship between local temperature gradients and local thermal conductivity (Figs 10–12), we observe a well-defined correlation between mean values of temperature gradients and mean values of reciprocal thermal conductivity for the main litho-chronological groups. Thus, variations in temperature gradients at depth greater than 100 m can be explained almost entirely by differences in thermal conductivity. At shallower depth, recent (past 100–150 years) climatic surface temperature increase (Cappelen 2012), introduces a significant transient effect resulting in reduced temperature gradients, and, at upper levels, even negative values are observed (Fig. 3, Fig. 5, Fig. 10 and Fig. 11). This transient effect penetrates to greater depths in boreholes with sandy sediments of high thermal diffusivity (Fig. 5A and 5B).

The correlation analysis shown in Fig. 12 also underlines the existence of a thermally conductive regime. Only locally, and generally at a very small scale, we observe temperature gradient perturbations caused by groundwater flow. If significant components of advective transfer of heat by groundwater migration were present, no such well-defined correlation between mean temperature gradients and mean conductivity, and consistent heat flow estimates, would be observed.

Regional and local temperature variations

With the present detailed information on thermal conductivity, temperature gradient variations and heat flow, we are able to discuss the observed local and regional temperature variations as displayed in Fig. 6.

The relatively high subsurface temperatures observed in eastern and southern Sjælland and Lolland are found in areas with carbonate rocks below a relatively thin cover of Quaternary deposits. In northern Jylland the subsurface temperatures are generally lower though similar carbonate rocks are found below the Quaternary deposits. This difference can most likely be explained by the fact that northern Jylland generally has slightly lower ground surface temperature and parts of the area are covered with greater thicknesses of Quaternary deposits, resulting in low temperature gradients.

The highest subsurface temperatures in Jylland are observed in areas with thick shallow deposits of Palaeogene clay of low thermal conductivity resulting in high temperature gradients as found in the Harre borehole (Fig. 3) and observed also at other locations with Palaeogene clays across Jylland (see Fig. 1). The lowest temperatures are often found in deep buried valleys with Quaternary deposits and in areas dominated by thick deposits of Miocene sand and silt, both characterised by relatively high thermal conductivities and low temperature gradients (Fig. 5A–C).

A distinct positive temperature anomaly is observed locally in the northernmost part of Salling, north-western Jylland. It is found in a 251 m deep borehole (DGU no 38.412) drilled into the top part of a salt diapir (the Batum structure, see Fig. 1 and Fig. 6). The high temperatures are associated with an exceptionally high heat flow of 91 mW/m^2 (Balling *et al*. 1981). Due to the high thermal conductivity of rock salt (Table 1), heat is led into the uppermost parts of salt structures, resulting in significantly higher heat flow and higher temperature gradients above salt diapirs (cf. numerical models by Balling *et al.* 1981; Jensen 1990).

At Stevns in the eastern part of Sjælland, temperatures, especially in the Stevns-1 borehole (DGU no. 218.1938; Fig. 5D) and in a nearby borehole (DGU no 217.724), are high compared with observations from boreholes in similar carbonate rocks in adjacent areas of Sjælland. Bonnesen *et al*. (2009) reported on a slow water flow upwards from two specific horizons in the Stevns-1 borehole. However, any slow upward water flow cannot alone explain the elevated temperatures (see Fig. 5D). Based on measured porosities of about 30% in the deeper parts of this borehole (Bonnesen *et al*. 2009) and a well-defined thermal conductivity-porosity relationship, determined in Balling *et al*. (1981, fig. 27), the thermal conductivity is estimated at c. 2.0 W/(m·K). With an observed temperature gradient of c. 3.0°C/100 m, we estimate the local heat flow to be c. 60 mW/m^2, much higher than the characteristic shallow heat flow discussed above. To understand this anomaly, further thermal observations and analysis in this area are needed.

Summary and conclusions

By compilation and analysis of all available information on measured borehole temperatures and rock thermal conductivity measurements from depths down to 300 m, we outline regional quantitative information on the shallow subsurface thermal structure for onshore Denmark.

At 50 m depth, the mean temperature (8.9 ± 0.8°C) has increased only little compared to the mean annual ground surface temperature. The higher mean values at 100 m (9.7 ± 1.1°C) and 200 m (11.6 ± 2.2°C), as well as a less representative mean of 14.9 ± 2.0°C at 300 m, reflect the general increase of temperatures with depth. In contrast to assumptions commonly held about only small lateral shallow temperature variations at specific depths, we observe significant variability both locally and regionally. Differences generally increase with depth. For depths of 100 and 200 m, we observe lateral variations (differences between lowest and highest observed temperatures) of 6 and 8°C, respectively. The variability is related to differences in thermal conductivity of the various lithologies.

Mean values of rock thermal conductivities for main lithologies lie within a range of 0.6–6 W/(m·K) (water saturated, at laboratory conditions), with the majority of values within the interval 1–3 W/(m·K). The content of quartz (with high conductivity) and rock porosity (holding water of low conductivity) are the main controlling factors.

Mean interval temperature gradients, divided in litho-chronological groups over which they are measured, vary significantly: -2–5°C/100 m in the depth interval 50–100 m and 0–5°C/100 m for depths > 100 m. At very shallow depths, less than 50 m, and often between 50 and 75 m as well, we observe very low gradients, locally also negative values (decreasing temperatures with depth). These low values reflect the depth penetration of recent climatic surface temperature increase. For deeper levels, we observe a well-defined inverse relationship between mean temperature gradients and mean thermal conductivity for the main lithologies. Quartz-rich sandy sediments (high thermal conductivity) have low mean temperature gradients (about 0.8–1.2°C/100 m); silty clay, limestone and chalk (intermediate conductivity) have intermediate mean gradients (about 1.6–2.5°C/100 m) and very fine-grained clay (low thermal conductivity) have high mean temperature gradients (about 3.3–4.3°C/100 m).

From a correlation plot of mean temperature gradient versus the reciprocal of associated mean thermal conductivity of the litho-chronological groups, we obtain a regional shallow heat flow estimate of 37 ± 5 mW/m^2. This low value is in good agreement with similarly low values from local site determinations using classical methods. Heat flow in the shallow subsurface is found to be around a factor of two lower than deep background heat flow. This is believed to be due to long-term palaeoclimatic effects primarily related to the significant increase in surface temperatures at the end of the last glaciation.

From our temperature and temperature gradient analysis, and from the above well-defined (inverse) correlation between temperature gradient variations and thermal conductivity variations, we conclude that the shallow subsurface thermal regime across the Danish area is largely controlled by thermal conduction. Generally, this applies both on local borehole scale and regionally. Only locally, and in rare cases, do we observe temperature and temperature gradient perturbations due to groundwater migration and in such cases with very small amplitudes.

In addition to general geoscientific purposes, our data and findings are important for several applica-

tions, such as exploitation of shallow geothermal energy and the use of the subsurface for heat storage and cooling purposes.

Acknowledgement

The data compilation, the majority of recent thermal conductivity measurements and temperature logging of shallow boreholes was funded by EUDP project grant 64011-0003 (Geoenergy. Closed loop boreholes - knowledge, tools and best practice). Inga Sørensen, Maria Pagola and Anne Mette Nielsen are thanked for their skilful laboratory work. We also thank Per Rasmussen, Steen Røj Jacobsen and Thue S. Bording for field assistance with borehole temperature logging and data processing. Reinhard Kirsch and an anonymous reviewer are thanked for their valuable comments.

References

Andersson, O. 2007: Aquifer Thermal Energy Storage (ATES). In: Paksoy, H.Ö. (ed.), Thermal Energy Storage for Sustainable Energy Consumption. NATO Science Series (Mathematics, Physics and Chemistry) 234, 155–176. Springer, Dordrecht.

Balling, N. 1979: Subsurface temperatures and heat flow estimates in Denmark. In: Čermák, V. & Rybach, L. (eds), Terrestrial Heat Flow in Europe, 161–171. Springer-Verlag, Berlin.

Balling, N. 1986: Temperature of geothermal reservoirs in Denmark. Report to Commission of the European Communities, contract EG-A-1-032-DK(G), 65 pp. Geophysical Laboratory, University of Aarhus.

Balling, N. 1992: Denmark. In: Hurtig, E., Haenel, R. & Zui, V. (eds), Geothermal Atlas of Europe, 25–28. Hermann Haack Verlagsgesellschaft, Gotha.

Balling, N. 2013: The lithosphere beneath Northern Europe: Structure and Evolution over Three Billion Years. Contributions from Geophysical Studies. Doctoral dissertation, 195 pp. Aarhus University.

Balling, N. & Bording, T.S. 2013: Temperatur, temperaturgradienter og varmeledningsevne i den geotermiske boring Sønderborg-1/1A. Scientific report, 12 pp. Department of Geoscience, Aarhus University.

Balling, N., Kristiansen, J., Breiner, N., Poulsen, K.D., Rasmussen, R. & Saxov, S. 1981. Geothermal measurements and subsurface temperature modelling in Denmark. Geoskrifter 16, 172 pp. Aarhus University.

Balling, N., Nielsen, S.B., Christiansen, H.S., Christensen, L.D. & Poulsen, S. 1992: The subsurface thermal regime and temperature of geothermal reservoirs in Denmark. Synthesis report to Commission of the European Communities, Contract EN3G-0029-DK, 89 pp. Department of Geoscience, Aarhus University.

Balling, N., Hvid, J.M., Mahler, A., Møller, J.J., Mathiesen, A., Bidstrup, T. & Nielsen, L.H. 2002: Denmark. In: Hunter, S. & Haenel, R. (eds), Atlas of Geothermal Resources in Europe. Publication No. EUR 17811 of the European Commission, 27–28, plate 15–16.

Balling, N., Poulsen, S.E., Fuchs, S., Mathiesen, A., Bording, T.S., Nielsen, S.B. & Nielsen, L.H. 2016: Development of a numerical 3D geothermal model for Denmark. In: Proceedings, European Geothermal Congress, Strasbourg, France, Sept 2016, 9 pp.

Bonnesen, E.P., Bøggild, O.B. & Ravn, J.P.J. 1913: Carlsbergfondets dybdeboring i Grøndals eng ved København 1894–1907 og dens videnskabelige resultater. Communications Geologiques, 105 pp. Muséum de Minéralogie et de Geologie de l'Université de Copenhague, Copenhagen.

Bonnesen, E.P., Larsen, F., Sonnenborg, T.O., Klitten, K. & Stemmerik, L. 2009: Deep saltwater in Chalk of North-West Europe: Origin, interface characteristics and development over geological time. Hydrogeology Journal 17, 1643–1663. doi:10.1007/s10040-009-0456-9

Bording, T.S., Nielsen, S.B. & Balling, N. 2019: Determination of thermal properties of materials by Monte Carlo inversion of pulsed needle probe data. International Journal of Heat and Mass Transfer 133, 154–165. doi:10.1016/j.ijheatmasstransfer.2018.12.104

Brigaud, F. & Vasseur, G. 1989: Mineralogy, porosity and fluid control on thermal conductivity of sedimentary rocks. Geophysical Journal International 98, 525–542. doi:10.1111/j.1365-246X.1989.tb02287.x

Buchardt, B. & Nielsen, A.T. 1985: Carbon and oxygen isotope composition of Cambro-Silurian limestone and anthraconite from Bornholm: Evidence for deep burial diagenesis. Bulletin of the Geological Society of Denmark 33, 415–435.

Buckley, D.K., Hinsby, K. & Manzano, M. 2001: Application of geophysical borehole logging techniques to examine coastal aquifer palaeohydrogeology. Geological Society, London, Special Publication 189, 251–270. doi:10.1144/GSL.SP.2001.189.01.15

Bullard, E.C. 1939: Heat Flow in South Africa. Proceedings of the Royal Society A: Mathematical, Physical and Engineering Sciences 173, 474–502. doi:10.1098/rspa.1939.0159

Cappelen , J. (ed.) 2012: Denmark – DMI Historical Climate Data Collection 1768–2011, Technical report 12-02, 90 pp. Danish Meteorological Institute.

Čermák, V. & Rybach, L. 1982: Thermal properties: Thermal conductivity and specific heat of minerals and rocks. In: Angeneister, G. (ed.), Landolt-Bornstein Numerical Data and Functional Relationships in Science and Technology, 305–343. Springer Verlag, Berlin, Heidelberg, New York.

Christensen, L. & Ulleberg, K. 1973: Sedimentology and micropalaeontology of the middle Oligocene sequence at Sofienlund, Denmark. Bulletin of the Geological Society of Denmark 22, 283–305.

Clauser, C. & Huenges, E. 1995: Thermal conductivity of rocks

and minerals. in: Ahrens, T.J. (ed.), Rock Physics and Phase Relations: A Handbook of Physical Constants. AGU Reference Shelf 3, 105–126. American Geophysical Union, doi:/10.1029/RF003p0105

Davis, M.G., Chapman, D.S., Van Wagoner, T.M. & Armstrong, P.A. 2007: Thermal conductivity anisotropy of metasedimentary and igneous rocks. Journal of Geophysical Research 112, B05216, 7 pp. doi:10.1029/2006JB004755

Ditlefsen, C. & Sørensen, I. 2014: D6 Overfladenære jordarters termiske egenskaber. Report to Energy technological development and demonstration program (EUDP), 23 pp. Geological Survey of Denmark and Greenland, Copenhagen. http://geoenergi.org/xpdf/d6_jordarters_termiske_egenskaber.pdf.

Ditlefsen, C., Sørensen, I., Slott, M. & Hansen, M. 2014: Estimating thermal conductivity from lithological descriptions – A new web-based tool for planning of ground-source heating and cooling. Geological Survey of Denmark and Greenland Bulletin 31, 55–58.

DMI 2018a: Klimanormaler [WWW Document]. URL http://www.dmi.dk/vejr/arkiver/normaler-og-ekstremer/klimanormaler-dk/ (accessed 12-7-2018).

DMI 2018b: Decadal mean weather [WWW Document]. URL http://www.dmi.dk/en/vejr/arkiver/decadal-mean-weather (accessed 17-7-2018).

Erlström, M., Boldreel, L.O., Lindström, S., Kristensen, L., Mathiesen, A., Andersen, M.S., Kamla, E. & Nielsen, L.H. 2018: Stratigraphy and geothermal assessment of Mesozoic sandstone reservoirs in the Øresund Basin – exemplified by well data and seismic profiles. Bulletin of the Geological Society of Denmark 66, 123–149.

GEUS 2017: Jupiter database [WWW Document]. URL http://www.geus.dk/DK/data-maps/jupiter/Sider/default.aspx (accessed 26-9-2017).

Gravesen, P. & Fredericia, J. 1984: ZEUS-geodatabasesystem. Borearkivet. Databeskrivelse, kodesystem og sideregistre. Danmarks Geologiske Undersøgelse Serie C, No 3, 259 pp.

Gravesen, P., Rolle, F. & Surlyk, F. 1982: Lithostratigraphy and sedimentary evolution of the Triassic, Jurassic and Lower Cretaceous of Bornholm, Denmark. Danmarks Geologiske Undersøgelse, Serie B 7, 51 pp.

Hansen, M. & Pjetursson, B. 2011: Free, online Danish shallow geological data. Geological Survey of Denmark and Greenland Bulletin 23, 53–56.

Heilmann-Clausen, C. 1995: Palæogene aflejringer over Danskekalken. Danmarks geologi fra Kridt til i dag. Aarhus Geokompendier 1, 69–114.

Heilmann-Clausen, C., Nielsen, O.B. & Gersner, F. 1985: Lithostratigraphy and depositional environments in the Upper Paleocene and Eocene of Denmark. Bulletin of the Geological Society of Denmark 33, 287–323.

Hellström, G. 2011: Borehole heat exchangers. In: Geotrainet Training Manual for Designers of Shallow Geothermal Systems, 31–52. GEOTRAINET, EFG, Brussels 2011.

Horai, K. 1971: Thermal conductivity of rock-forming minerals. Journal of Geophysical Research 76, 1278–1308. doi:10.1029/JB076i005p01278

Houmark-Nielsen, M. 1988: Pleistocene stratigraphy and glacial history of the central part of Denmark. Bulletin of the Geological Society of Denmark 36, 1–189.

Houmark-Nielsen, M. 2004: The Pleistocene of Denmark: A review of stratigraphy and glaciation history. In: Ehlers, J. & Gibbard, P.L. (eds), Quaternary Glaciations 5 – Extent and Chronology, 35–46. Developments in Quaternary Science. Elsevier, doi:10.1016/S1571-0866(04)80055-1

Håkansson, E. & Pedersen, S.A.S. 1992: Geologisk kort over den danske undergrund. Varv.

Jacobsen, E.M. 1985: En råstofgeologisk kortlægning omkring Roskilde. Dansk Geologisk Forening, Årsskrift for 1984, 65–78.

Jensen, P.K. 1990: Analysis of the temperature field around salt diapirs. Geothermics 19, 273–283. doi:10.1016/0375-6505(90)90047-F

Jørgensen, F. & Sandersen, P.B.E. 2006: Buried and open tunnel valleys in Denmark – erosion beneath multiple ice sheets. Quaternary Science Reviews 25, 1339–1363. doi:10.1016/j.quascirev.2005.11.006

Knudsen, P. 1983: Bestemmelse af geotermiske parametre indenfor den årlige temperaturvariations virkningsområde. MSc. thesis. Department of Geoscience, Aarhus University.

Kristiansen, J.I. 1982: The transient cylindrical probe method for determination of thermal parameters and earth material. Geoskrifter 18, 154 pp. Aarhus University.

Kristiansen, J., Saxov, S., Balling, N. & Poulsen, K. 1982: *In situ* thermal conductivity measurements of Precambrian, Palaeozoic and Mesozoic rocks on Bornholm, Denmark. Geologiska Föreningens i Stokholm Förhandlingar 104, 49–56.

Kukkonen, I.T. & Jõeleht, A. 2003: Weichselian temperatures from geothermal heat flow data. Journal of Geophysical Research 108, paper 2163, 11 pp. doi:200310.1029/2001JB001579

Larsen, G., Jørgensen, F.H. & Priisholm, S. 1977: The stratigraphy, structure and origin of glacial deposits in the Randers area, eastern Jylland. Danmarks Geologiske Undersøgelse II. Række 111, 36 pp.

Larsen, N.K., Knudsen, K.L., Krohn, C.F., Kronborg, C., Murray, A.S. & Nielsen, O.B. 2009: Late Quaternary ice sheet, lake and sea history of southwest Scandinavia – A synthesis. Boreas 38, 732–761. doi:10.1111/j.1502-3885.2009.00101.x

Major, M., Poulsen, S.E. & Balling, N. 2018: A numerical investigation of combined heat storage and extraction in deep geothermal reservoirs. Geothermal Energy 6 (1), 16 pp. doi:10.1186/s40517-018-0089-0

Mathiesen, A., Kristensen, K., Bidstrup, T. & Nielsen, L.H. 2009: Vurdering af det geotermiske potentiale i Danmark. Danmarks og Grønlands Geologiske Undersøgelse Rapport 2009/59, 30 pp. Copenhagen.

Mathiesen, A., Nielsen, L.H. & Bidstrup, T. 2010: Identifying potential geothermal reservoirs in Denmark. Geological Survey of Denmark and Greenland Bulletin 20, 19–22.

Michelsen, O., Nielsen, L.H., Johannessen, P.N., Andsbjerg, J. & Surlyk, F. 2003: Jurassic lithostratigraphy and stratigraphic development onshore and offshore Denmark. Geological

Survey of Denmark and Greenland Bulletin 1, 147–216.
Møller, I., Søndergaard, V.H. & Jørgensen, F. 2009a: Geophysical methods and data administration in Danish groundwater mapping. Geological Survey of Denmark and Greenland Bulletin 17, 41–44.
Møller, I., Søndergaard, V.H., Jørgensen, F., Auken, E. & Christiansen, A.V. 2009b: Integrated management and utilization of hydrogeophysical data on a national scale. Near Surface Geophysics 7, 647–659. doi:10.3997/1873-0604.2009031
Møller, I., Balling, N., Bording, T.S., Vignoli, G. & Rasmussen, P. 2014: D9 Temperatur og temperaturgradienter ved og under jordoverfladen i relation til lithologi. Report to Energy technological development and demonstration program (EUDP), 47 pp. Geological Survey of Denmark and Greenland, Copenhagen. http://geoenergi.org/xpdf/d9-temperatur_og_temperaturgradienter.pfd.
Nielsen, A.T. & Schovsbo, N.H. 2007: Cambrian to basal Ordovician lithostratigraphy in Southern Scandinavia. Bulletin of the Geological Society of Denmark 53, 47–92.
Nielsen , O.B. (ed.) 1994: Lithostratigraphy and biostratigraphy of the Tertiary sequence from the Harre borehole, Denmark, 168 pp. Department of Earth Sciences, Aarhus University.
Nielsen, S.B., Balling, N. & Christiansen, H.S. 1990: Formation temperatures determined from stochastic inversion of borehole observations. Geophysical Journal International 101, 581–591.
Pagola, M.A. 2013: Investigation of Soil for Shallow Geothermal Energy Systems - Field tests and laboratory measurements for the determination of thermal properties for the design of combined abstraction of heat and storage of solar energy. MSc thesis, 100 pp. VIA University College, Horsens.
Pedersen, G.K. & Surlyk, F. 1983: The Fur Formation, a late Paleocene ash-bearing diatomite from northern Denmark. Bulletin of the Geological Society of Denmark 32, 43–65.
Porsvig, M. 1986: Varmeovergangsforhold omkring jordslanger. Energiministeriets varmepumpeforskningsprogram 33, 56 pp.
Poulsen, S.E., Balling, N., Bording, T.S., Mathiesen, A. & Nielsen, S.B. 2017: Inverse geothermal modelling applied to Danish sedimentary basins. Geophysical Journal International 211, 188–206. doi:10.1093/gji/ggx296
Powell, W.G., Chapman, D.S., Balling, N. & Beck, A.E. 1988: Continental heat-flow density. In: Haenel, R., Rybach, L. & Stegena, L. (eds), Handbook of Terrestrial Heat-Flow Density Determination, 167–222. Kluwer Academic Publishers, Dordrecht.
Rasmussen, E.S., Dybkjær, K. & Piasecki, S. 2010: Lithostratigraphy of the Upper Oligocene – Miocene succession of Denmark. Geological Survey of Denmark and Greenland Bulletin 22, 1–92.
Rasmussen, P., Højberg, A.L. & Ditlefsen, C. 2016: 3D modelling of borehole heat exchangers at hydrogeological conditions typical of the north European lowlands, sensitivity studies from Denmark. Proceedings, European Geothermal Congress, Strasbourg, France, 19–24 Sept 2016, 5 pp.
Robertson, E.C. 1988: Thermal Properties of Rocks. Open-File Report 88-441, 106 pp. US Geological Survey.
Røgen, B., Ditlefsen, C., Vangkilde-Pedersen, T., Nielsen, L.H. & Mahler, A. 2015: Geothermal energy use, 2015 country update for Denmark. Proceedings, World Geotermal Congress 2015, Melbourne, Australia, 19–25 April 2015, 9 pp.
Sandersen, P.B.E. & Jørgensen, F. 2017: Buried tunnel valleys in Denmark and their impact on the geological architecture of the subsurface. Geological Survey of Denmark and Greenland Bulletin 38, 13–16.
Sanner, B. 2016: Shallow geothermal energy – history, development, current status, and future prospects. Proceedings, European Geothermal Congress, Strasbourg, France, 19–24 Sept 2016, 19 pp.
Scharling, M. 2012: Climate Grid, Denmark. Datset for use in research and education. Daily and monthly values 1989–2010, 10×10 km precipitation sum, 20×20 km avarage temperature, accumulated potential evaporation (Makkink), average wind speed, accumulated global radiation. Technical report 12-10, 12 pp. Danish Meteorological Institute, Copenhagen.
Somerton, W.H. 1992: Thermal properties and temperature-related behavior of rock/fluid systems. Developments in Petroleum Science 37, 1st ed, 256 pp. Elsevier, Amsterdam.
Surlyk, F., Rasmussen, S.L., Boussaha, M., Schiøler, P., Schovsbo, N.H., Sheldon, E., Stemmerik, L. & Thibault, N. 2013: Upper Campanian–Maastrichtian holostratigraphy of the eastern Danish Basin. Cretaceous Research 46, 232–256. doi:10.1016/j.cretres.2013.08.006
Thomsen, E. 1995: Kalk og kridt i den danske undergrund. Danmarks geologi fra Kridt til i dag. Aarhus Geokompendier 1, 31–67.
Vangkilde-Pedersen, T., Ditlefsen, C. & Højberg, A.L. 2012: Shallow geothermal energy in Denmark. Geological Survey of Denmark and Greenland Bulletin 26, 37–40.
Von Herzen, R. & Maxwell, A.E. 1959: The measurement of thermal conductivity of deep-sea sediments by a needle probe method. Journal of Geophysical Research 64, 1557–1563. doi:doi/10.1029/JZ064i010p01557
Waight, T.E., Frei, D. & Storey, M. 2012: Geochronological constraints on granitic magmatism, deformation, cooling and uplift on Bornholm, Denmark. Bulletin of the Geological Society of Denmark 60, 23–46.
Waples, D.W. & Waples, J.S. 2004: A Review and Evaluation of Specific Heat Capacities of Rocks, Minerals, and Subsurface Fluids. Part 1: Minerals and Nonporous Rocks. Natural Resources Research 13, 97–122. doi:10.1023/B:NARR.0000032647.41046.e7
Weibel, R., Olivarius, M., Kristensen, L., Friis, H., Leth, M., Kjøller, C., Mathiesen, A. & Nielsen, L.H. 2017: Predicting permeability of low-enthalpy geothermal reservoirs: A case study from the Upper Triassic – Lower Jurassic Gassum Formation, Norwegian – Danish Basin. Geothermics 65, 135–157. doi:10.1016/j.geothermics.2016.09.003
York, D., Evensen, N.M., Martínez, M.L. & De Basabe Delgado, J. 2004: Unified equations for the slope, intercept, and standard errors of the best straight line. American Journal of Physics 72, 367–375. doi:10.1119/1.1632486

Appendix A. Summary statistics of thermal conductivities for litho-chronological groups in Fig. 2, also shown in Fig. 8. Individual data are available from Supplementary data file 2.

Litho-chronological group	Number of localities	Number of samples	Mean of mean W/(m·K)	Min. W/(m·K)	Max. W/(m·K)
Quaternary gytja	1	3	0.68	0.58	0.86
Quaternary marine sand	2	5	1.77	1.48	1.96
Quaternary marine clay	3	4	1.21	1.04	1.42
Quaternary meltwater sand	8	13	2.31	1.98	2.93
Quaternary meltwater clay	4	8	1.62	0.92	2.26
Quaternary sand till	1	2	2.05	1.96	2.14
Quaternary clay till	10	29	2.10	1.40	2.70
Miocene quartz sand	2	4	2.65	2.35	3.34
Miocene mica sand	3	4	1.82	1.70	1.90
Miocene mica silt	2	9	1.30	1.00	1.48
Miocene mica clay	5	8	1.29	0.90	1.74
Oligocene clay	6	30	1.15	0.80	1.48
Eocene clay	4	8	1.03	0.80	1.40
Eocene diatomite	1	3	0.63	0.61	0.67
Paleocene clay	3	12	1.02	0.78	1.40
Danian limestone	3	5	1.51	0.90	2.10
Maastrichtian chalk	7	41	1.67	1.45	1.98
Jurassic sand and sandstone	3	7	2.62	2.26	2.84
Jurassic clay	1	1	1.34	1.34	1.34
Jurassic thin beds of sand and clay	4	4	1.95	1.88	2.04
Ordovician Komstad limestone	1	7	2.75	2.70	2.82
Cambrian alum shale	1	2	1.69	1.67	1.70
Cambrian Broens Odde Member	2	4	4.11	3.88	4.29
Cambrian Balka sandstone	1	1	6.12	6.12	6.12
Cambrian Nexø sandstone	1	7	4.51	4.21	4.99
Precambrian crystalline rocks	11	39	3.07	2.57	3.68

Appendix B. Summary statistics of the temperature gradients displayed in Fig. 10 and Fig. 11. Temperature gradients are divided in litho-chronological groups (Fig. 2) and in two depth intervals (50–100 m and >100 m depth).

	Litho-chronological group	Number of wells	Number of samples	Mean °C/(100 m)	Std.dev. °C/(100 m)	Min. °C/(100 m)	Max. °C/(100 m)
50–100 m depth	**Quarternary deposits**	24	347	0.90	0.99	-2.83	5.08
	Meltwater sand & gravel	10	76	0.56	0.80	-1.22	2.31
	Clay till	3	16	1.91	0.83	0.88	3.16
	Meltwater clay	5	30	1.05	1.06	0.11	5.08
	Marine clay	2	18	1.54	1.08	0.35	2.76
> 100 m depth	**Quarternary deposits**	12	280	1.49	0.82	0.04	3.43
	Meltwater sand & gravel	9	152	1.19	0.62	0.14	2.96
	Clay till	0	0	-	-	-	-
	Meltwater clay	0	0	-	-	-	-
	Marine clay	1	4	1.80	0.33	1.33	2.21
50–100 m depth	**Neogene deposits**	6	116	1.08	0.64	-1.21	2.60
	Miocene quartz sand and gravel	1	2	-0.71	0.49	-1.21	-0.22
	Miocene mica sand	2	16	0.51	0.65	-0.23	1.23
	Miocene mica silt	1	6	1.55	0.03	1.50	1.58
	Miocene mica clay	4	38	1.37	0.70	0.28	2.60
> 100 m depth	**Neogene deposits**	9	299	1.55	0.52	0.53	2.97
	Miocene quartz sand and gravel	1	2	0.86	0.06	0.80	0.92
	Miocene mica sand	1	25	1.66	0.41	1.13	2.28
	Miocene mica silt	3	33	1.80	0.40	1.18	2.43
	Miocene mica clay	5	90	1.68	0.55	0.54	2.97
50–100 m depth	**Palaeogene clastic deposits**	8	98	2.49	0.67	0.47	3.51
	Oligocene clay	2	19	2.64	0.51	1.77	3.25
	Oligocene thin beds of clay, silt and sand	1	17	2.23	0.85	0.47	3.22
	Eocene Søvind marl	2	26	2.84	0.37	2.22	3.46
	Eocene clay	0	0	-	-	-	-
	Eocene thin beds of clay, silt and sand	0	0	-	-	-	-
	Selandian clay	3	26	2.13	0.64	1.20	3.14
> 100 m depth	**Palaeogene clastic deposits**	8	246	3.48	0.71	1.78	4.67
	Oligocene clay	3	59	3.77	0.33	3.10	4.41
	Oligocene thin beds of clay, silt and sand	2	31	3.46	0.16	3.15	3.66
	Eocene Søvind marl	1	3	2.46	0.07	2.36	2.52
	Eocene clay	1	31	4.30	0.24	3.94	4.64
	Eocene thin beds of clay, silt and sand	1	15	3.29	0.41	2.12	3.56
	Selandian clay	5	24	3.30	0.49	2.63	3.89
50–100 m depth	**Pal. & u. Maastrichtian carbonate deposits**	12	189	1.97	1.03	0.35	5.37
	Selandian limestone	0	0	-	-	-	-
	Danian limestone	5	23	1.90	1.06	0.47	3.59
	Maastrichtian & Campanian chalk	8	121	2.10	1.08	0.35	5.08
> 100 m depth	**Pal. & u. Maastrichtian carbonate deposits**	14	696	2.37	0.69	0.21	4.38
	Selandian limestone	1	24	2.18	0.23	1.78	2.70
	Danian limestone	5	83	2.20	0.38	1.32	3.31
	Maastrichtian & Campanian chalk	9	453	2.47	0.78	0.21	4.38
50–100 m depth	**Lower Cretaceous and Jurassic**	6	88	1.27	0.67	0.15	2.76
	Sand and sandstone	3	38	1.57	0.66	0.84	2.76
	Clay and claystone	1	1	1.23	0.00	1.23	1.23
	Thin beds of clay, silt and sand	1	13	1.09	0.25	0.77	1.42
> 100 m depth	**Lower Cretaceous and Jurassic**	3	123	1.32	0.29	0.90	2.44
	Sand and sandstone	3	44	1.26	0.25	0.90	1.63
	Clay and claystone	1	3	1.31	0.04	1.26	1.34
	Thin beds of clay, silt and sand	1	25	1.61	0.34	1.22	2.44
50–100 m depth	**Cambrian and Precambrian rocks**	4	34	0.99	0.22	0.58	1.24
	Cambrian sandstone	2	13	0.84	0.15	0.72	1.15
	Crystalline rocks	2	19	1.17	0.04	1.07	1.24
> 100 m depth	**Cambrian and Precambrian rocks**	0	0	-	-	-	-
	Cambrian sandstone	0	0	-	-	-	-
	Crystalline rocks	0	0	-	-	-	-